Vaccine Supply Chains in Resource-Limited Settings: Mitigating the Impact of Rainy Season Disruptions

KU LEUVEN

FACULTEIT ECONOMIE EN BEDRIJFSWETENSCHAPPEN

Vaccine Supply Chains in Resource-Limited Settings: Mitigating Rainy Season Disruptions

Kim DE BOECK
Catherine DECOUTTERE
Jónas ODDUR JÓNASSON
and Nico VANDAELE

KBI_2002

Vaccine Supply Chains in Resource-Limited Settings: Mitigating Rainy Season Disruptions

Kim De Boeck*

Research center for access-to-medicines, KU Leuven, Belgium, kim.deboeck@kuleuven.be

Catherine Decouttere

Research center for access-to-medicines, KU Leuven, Belgium, catherine.decouttere@kuleuven.be

Jónas Oddur Jónasson

MIT Sloan School of Management, Massachusetts Institute of Technology, Cambridge, Massachusetts, joj@mit.edu

Nico Vandaele

Research center for access-to-medicines, KU Leuven, Belgium, nico.vandaele@kuleuven.be

Abstract

Immunization is widely recognized as one of the most successful and cost-effective health interventions, preventing two to three million deaths from vaccine-preventable diseases each year. Although progress has been made in recent years, substantial operational challenges persist in resource-limited settings with frequent stock-outs contributing to sub-optimal immunization coverage and inequality in vaccine access. In this paper, we investigate the role of rainy season induced supply chain disruptions on vaccination coverage and inequalities. We develop a modeling framework combining spatial modeling—to predict flood disruptions in road networks—and a discrete-event simulation of a multi-tiered vaccine supply chain (VSC). Our models are fitted and validated using data from the Malagasy VSC network. Our baseline simulation predicts the national vaccination coverage with good accuracy and suggests that 67% of regions with low reported immunization coverage are affected by rainy season disruptions or operational inefficiencies, causing significant geographical inequalities in vaccine access. We investigate various mitigation strategies to increase the resiliency of VSCs and find that by strategically placing buffer inventory at targeted facilities prior to the rainy season the proportion of children receiving all basic vaccines in these areas is increased by 7% and the geographical inequality in vaccination coverage is reduced by 11%. By also

*Corresponding author.

increasing the replenishment frequency from every third month to every month, the national vaccination coverage improves by 37%. Our results contribute to achieving the UN Sustainable Development Goals (SDGs) by providing actionable insights for improving vaccination coverage (SDG 3) and investigating the resiliency of the VSC to increased flooding due to climate change (SDG 13).

Keywords: Global Health; Vaccine Supply Chain Design; Resource-Limited Settings; UN Sustainable Development Goals; Spatial Modeling; Discrete-Event Simulation

1 Introduction

The third goal of the United Nations (UN) Sustainable Development Goals (SDGs) is to "ensure healthy lives and promote well-being for all at all ages" (UN, 2019b). Immunization is widely recognized as one of the world's most successful and cost-effective health interventions, preventing two to three million deaths each year from vaccine-preventable diseases (WHO, 2017).

Although immunization coverage has improved in recent years, substantial challenges persist. First, immunization coverage rates are too low (UN, 2019b). Global coverage of the pneumococcal conjugate vaccine, which has the potential to substantially reduce under five mortality rates, is below 50%. Coverage of the required two doses of the measles vaccine increased from 59% in 2015 to 67% in 2017, but is still short of the 95% threshold needed to prevent outbreaks of this highly contagious disease. While coverage of the three required doses of DTP (the vaccine preventing diphtheria, tetanus and pertussis) increased from 72% in 2000 to 85% in 2015, it has remained unchanged between 2015 and 2017. Second, immunization access is demographically and geographically unequal. Immunization coverage is substantially lower in low- and middle-income countries (LMICs) than in high-income countries (WHO/UNICEF, 2017). Furthermore, immunization coverage inequalities favoring rich and urban populations within LMICs have been reported (Restrepo-Méndez et al., 2016).

A main driver of poor immunization coverage in LMICs is the inability of vaccine supply chains (VSCs) to ensure the availability of vaccines at the administration points (Aina et al., 2017). An important contributing factor to the vaccine distribution challenge is the presence of a rainy season, during which facilities are cut off from the road network. According to the World Health Organization (WHO), floods and extreme precipitation are increasing in frequency and intensity, further disrupting the supply of medical and health services (WHO,

2018). Moreover, the impact of the rainy season will likely increase in the future due to climate change, disproportionally affecting LMICs with weak health infrastructure. While SDG 13 (UN, 2019a) aims to strengthen resiliency to climate-related hazards and advance climate change mitigation and impact reduction, limited research exists on improving supply chain resiliency to rainy season disruptions. The want of prior work in this area is likely due to the lack of data (reliable data on road networks, VSC disruptions due to flooding, and the geographical distribution of demand are not readily available) and a modeling framework to describe the impact of the rainy season on supply chain performance.

In this paper, we develop a data-driven modeling approach combining spatial modeling and discrete-event simulation to assess and mitigate the effect of the rainy season on vaccination coverage and inequalities in LMICs, and we apply it to the Malagasy VSC, using data provided by our field collaborators at UNICEF Madagascar. Our discrete-event simulation model captures the important characteristics and challenges inherent to VSCs in LMICs, including transportation capacity and potential cold chain breakdowns. Furthermore, we leverage geographic information systems (GIS) and spatial modeling to overcome the lack of data, allowing us to predict realistic estimates for the road network, the parts of the supply chain network that are likely to be disrupted during the rainy season, and the geographical distribution of demand. While we apply our modeling framework to the Malagasy VSC, its structure is general and representative of VSCs in other LMICs, many of which routinely face disruptions caused by a rainy season. As a result, our insights and mitigation strategies are applicable beyond the case of Madagascar.

We use our modeling framework to address three main questions. First, what are the key drivers behind the public health performance of the Malagasy VSC? Specifically, what is the impact of rainy season disruptions and the current operational strategy on vaccination coverage and inequalities? Second, how effective are simple, shorter-term modifications to the Malagasy VSC operations to improve the health outcomes (i.e., vaccination coverage, inequalities) of the current system and to mitigate the effect of the rainy season? Third, how sensitive is the performance of the current VSC, as well as the proposed mitigation strategies, to increased disruptions due to climate change?

Our simulation of the current system uncovers two main drivers of low vaccination coverage within the VSC. First, using our spatial modeling framework we are able to identify the facilities which are most likely to be impacted by the rainy season disruptions. Our estimates indicate

that vaccination coverage is on average 27 percentage points lower in those facilities that are affected by the rainy season, confirming that rainy season disruptions in the VSC are a main driver of unequal access to vaccines. Second, we find that missed orders are a much larger source of operational inefficiency in the Malagasy VSC than wasted vials due to cold chain or transportation breakdowns. Furthermore, the missed orders are not only due to upstream stockouts but also due to limited transportation capacity. We explore various operational strategies to mitigate the impact of the rainy season. We find that while increasing the order-up-to levels at facilities affected by the rainy season results in a modest improvement in vaccination coverage (3 percentage points for facilities impacted by the rainy season, 1 percentage point nationally), the full potential of the rainy season mitigation strategy is only realized when the underlying operational bottlenecks in the VSC are concurrently addressed. By jointly increasing the VSC's transportation capacity (through increased replenishment frequency), the vaccination coverage of facilities affected by the rainy season can be increased by 29 percentage points (accompanied by a 23 percentage point increase in the national vaccination coverage). Finally, we find that a relatively mild increase in flooding, due to climate change, would result in 37% more facilities being affected. Although the mitigation strategy of jointly increasing transportation frequency and order-up-to levels at the affected facilities is still effective, it cannot prevent some deterioration in vaccination coverage. More substantial action is therefore required to make the VSC robust to climate change.

Our work makes practical-, academic-, and policy-relevant contributions. Practically, we provide concrete suggestions for improving the VSC in Madagascar. Furthermore, VSCs in most other countries in sub-Saharan Africa (SSA) are also assisted by UNICEF and have a similar structure. Therefore, our results are applicable to inform VSC design beyond Madadascar. From an academic perspective, we propose a modeling framework combining discrete-event simulation modeling with state-of-the art spatial modeling to estimate the road network and the geographical distribution of demand, and to predict supply chain disruptions due to the rainy season and increased flooding due to climate change. The use of GIS and spatial modeling provides an opportunity for the humanitarian and global health operations management community, as it allows researchers to obtain realistic estimates of geographical data that are often unavailable. Finally, this work contributes to the SDGs in several ways. Assessing and improving vaccination coverage and inequalities (induced by the rainy season) contributes to reducing preventable deaths of newborns and children under five years of age (SDG 3.2) as well

as to provide access to vaccines for all (SDG 3.8) (UN, 2019b). Investigating and understanding the potential impact of increased flooding due to climate change contributes to improving resiliency to climate-related hazards (SDG 13.1) and to raising awareness on climate change mitigation and impact reduction (SDG 13.3) (UN, 2019a).

The remainder of this paper is organized as follows. We review the existing related literature in Section 2, and provide background information on VSCs in LMICs and the case of Madagascar in Section 3. Our data-driven modeling approach combining spatial modeling and discrete-event simulation is discussed and validated in Section 4. Results and policy insights are reported in Section 5, and Section 6 presents concluding remarks including a summary of the main insights, a discussion of the limitations of this study, and opportunities for future work.

2 Related literature

Kraiselburd and Yadav (2012) state that ineffective and poorly designed supply chains for purchasing and distributing medicines, vaccines, and health technologies are one of the most important barriers to increasing access in LMICs, and they indicate the potential contribution of the operations management research community in these settings. Our work contributes to the growing body of literature on global and public health operations management, including not-for-profit and development operations.

This includes work regarding the impact of donor funding on inventory management (Natarajan and Swaminathan, 2014), inventory allocation (Natarajan and Swaminathan, 2017) and national stock-outs of life-saving drugs (Gallien et al., 2017), the estimation and measurement of managerial efficiency drivers of country-level health care programs (Berenguer et al., 2016), the location of health facilities and planning of health schemes in rural areas (Smith et al., 2009), and the location and routing of mobile health clinics (Doerner et al., 2007) in LMICs. Furthermore, Leung et al. (2016) investigate the impact of inventory management on stock-outs of essential drugs in health clinics in Zambia, thereby indicating that more rigorous, independent research on pharmaceutical supply chains in LMICs is needed. In addition, McCoy and Lee (2014) model the impact of increasing the capacity of the health delivery fleet in Zambia on efficiency and equity. The global and public health operations literature also includes studies that aim to improve several aspects of tuberculosis and HIV supply chains such as improving HIV early infant diagnosis supply chains (Deo and Sohoni, 2015; Jónasson et al., 2017), locating roadside clinics

in Africa to improve access to HIV related services for long distance truck drivers (Ares et al., 2016; de Vries et al., 2020), and allocating scarce resources for planning treatment programs while explicitly incorporating adherence (Mccoy and Johnson, 2014). Furthermore, de Treville et al. (2006) illustrate how basic principles of operations management can assist not-for-profit organizations by presenting a case study in which they assess the impact of long lead times on the efforts of the WHO to eradicate tuberculosis. Another stream of papers focuses on the malaria supply chain by designing strategies to improve the distribution of malaria medications (Parvin et al., 2017) and by investigating whether donors should subsidize the purchases and/or the sales of the private-sector distribution channel to improve access to malaria drugs (Taylor and Xiao, 2014). In global and public health settings, community health workers often play an important role. In this regard, Cherkesly et al. (2019) investigate the design of a network of community health workers in underserved areas. Whereas all of the above studies focus on the supply side, Mehrotra and Natarajan (2019) incorporate both supply and demand in their analysis by allocating a limited budget to patient and provider incentives to maximize health outcomes in humanitarian health care service programs.

A last stream of papers that is related to global and public health operations, and that is most closely linked to our study, focuses on VSCs in LMICs (see De Boeck et al. (2019) for a detailed review). Most closely linked to our paper are studies that investigate the impact of altering shipping policies and frequencies (Assi et al., 2013; Brown et al., 2014), and the effect of implementing different ordering policies combined with various buffer stock levels (Rajgopal et al., 2018). Moreover, Haidari et al. (2016) and Rabta et al. (2018) explore the impact of operating drones and indicate their potential, especially for addressing last mile distribution problems. Approaching immunization systems from a broader, system-wide perspective, Decouttere et al. (2020) capture the complexity of immunization systems by mapping the different subsystems and their links to the SDGs. The main differentiating factors of our work are its focus on the impact of the rainy season, and the combination of spatial modeling and discrete-event simulation. Moreover, we incorporate several characteristics inherent to VSCs that are not or only sporadically considered in the current literature on VSCs (e.g., unreliable cold chain equipment, stochastic transportation times) (De Boeck et al., 2019).

3 Vaccine supply chains in LMICs and the case of Madagascar

In this section, we provide some background information on VSCs in LMICs (Section 3.1) and we introduce the case of Madagascar (Section 3.2).

3.1 Background on vaccine supply chains in LMICs

VSCs in LMICs mainly consist of four components (De Boeck et al., 2019): sourcing of vaccines at the central (i.e., national) level, storage of vaccines at the storage facilities, transportation of vaccines between levels, and administration of vaccines at the administration points. In the remainder of this subsection, we give a brief overview of each of these components. For a detailed overview and comprehensive review of vaccine distribution networks in LMICs, we refer to De Boeck et al. (2019) and references therein.

Initially, vaccines are shipped from the manufacturer to the destination country. Often, health and humanitarian organizations, including the WHO, UNICEF, the Pan American Health Organization (PAHO), and the Global Alliance for Vaccines and Immunization (GAVI), provide assistance during the procurement process by identifying qualified vaccines and manufacturers, and by ensuring affordable prices (Herlin and Pazirandeh, 2012).

Throughout the VSC, vaccines are stored at different storage locations. Given the required low temperatures during storage, appropriate cold chain equipment (CCE) is needed. In LMICs, the requirement of CCE for storage introduces multiple challenges: CCE is often unreliable due to equipment failures, power outages and an unreliable electricity grid; preventive maintenance to avoid equipment failures is rarely executed; spare parts are often not available; and repair of CCE can take months (Ashok et al., 2017; Brooks et al., 2017; Karp et al., 2015; Lennon et al., 2017). In addition, storage space at the facilities is limited and in practice sometimes needs to be shared among vaccines and other temperature-sensitive products.

Transportation of vaccines between the facilities is done using a variety of transportation modes (e.g., airplanes, trucks, motorcycles, bicycles, carrying vaccines on foot) depending on the road conditions and the accessibility of the facilities. Distributing vaccines in LMICs also poses several challenges: transportation durations are stochastic due to transportation disruptions including bad road conditions, possibility of vehicle ransacking and vehicle issues; remote areas can be very hard to reach; and vaccines need to be kept cold during transportation, resulting in the requirement of adequate CCE for distribution (Lemmens et al., 2016).

The final component of the VSC is the actual administration of the vaccines. An important form of wastage encountered in this step is open-vial wastage which occurs when a multi-dose vial is opened, but not all doses are administered. Since several multi-dose vials cannot be used anymore six hours after opening, the remainder of doses in a multi-dose vial at the end of a vaccination session is discarded, and thus results in open-vial wastage (WHO, 2014). It is important to note the difference between a vaccine dose and a vaccine vial. To administer one vaccination to a child, one vaccine dose is needed. A vaccine vial is a unit that can contain one or multiple doses. This means that for a ten-dose vial with open-vial wastage, a daily demand of one or ten doses results in the same number of demanded vials (i.e., one vial). Depending on the vaccine, vaccine vials can be single- or multi-dose. The smallest unit possible to transport or store is thus a vaccine vial (possibly containing multiple doses). General policy states that after depleting a multi-dose vial, a new vial should be opened upon a patient arrival (Heaton et al., 2017), meaning that every arriving patient gets vaccinated if enough vaccines are available.

VSCs in LMICs face high percentages of wastage. In addition to open-vial wastage occurring at the administration step, a second type of wastage comprises closed-vial wastage. Closed-vial wastage results from unreliable storage and distribution equipment, and limited shelf life (e.g., vaccines that have been out of the required temperature ranges, vaccine vials broken or lost during storage or transportation) (Wallace et al., 2017).

3.2 The Malagasy vaccine supply chain

The current VSC of Madagascar is representative of VSCs in the region and has a similar structure as described in Section 3.1. The Malagasy VSC consists of four levels: one national facility in Antananarivo, 22 regional facilities, 106 district facilities and 3155 basic health centers. The national facility receives vaccines from the manufacturer through UNICEF, our field collaborator. These national deliveries are scheduled to take place four times per year. Next, from the national facility, there are two ways in which vaccines can flow through the network to the district level. First, in the standard way, shipments from the national to the regional facilities occur on a trimestral basis through (cold) trucks or airplanes. These vaccines are then transported from the regional to the district level through trimestral deliveries by pick-ups or motorcycles. Second, a selected few district facilities are replenished directly by the national facility by means of (cold) trucks or airplanes. This is the case for district facilities that are either close to an existing transportation route or that are geographically isolated. Finally,

vaccines are picked up monthly from the district facilities by the basic health centers (which serve as vaccination points).

The Malagasy VSC faces numerous challenges. Similar to other LMICs, it has a high percentage of obsolete CCE and vaccine wastage. Also, the existing road network is in poor condition as it is the 5th worst in the world according to the World Economic Forum (2017). In addition, getting the required vaccines to the targeted population in Madagascar is further complicated by the presence of a rainy season. During the rainy season (from November to March), the accessibility of the affected transportation links is reduced or eliminated, resulting in numerous facilities that are seasonally isolated for months at a time. According to the World Bank (2015), rain-related issues (i.e., floodings, cyclones, late rains) accounted for 26.6% of the negative shocks reported in 2010 in Madagascar. Moreover, sea levels will rise in the future due to climate change, increasing the number of transportation links and facilities affected by the rainy season (USAID, 2017). The World Bank reports that "Madagascar is one of the most climate vulnerable countries in the world with a poor and predominantly rural population, a high geographical exposure to climate events, and a lack of readily available resources to respond to and recover from natural disasters" and predicts that the potential future impact of extreme precipitation and flooding, and sea level rise on health services in Madagascar is alarmingly high (World Bank, 2015).

Moreover, Madagascar experiences major inequities in immunization coverage, which are mainly geographic in nature. A study done by van den Ent et al. (2017) indicates that a child living in a more wealthy region of Madagascar is 3.4 times more likely to be vaccinated than a child living in a poorer region characterized by remote areas located far away from access to health care. Also, the World Bank stated in 2015 that "almost 30 percent of all deaths in Madagascar are still attributable to preventable and infectious and parasitic diseases, with the burden of disease falling disproportionately on the poor" and that "immunization is a proxy indicator of the availability of primary health care in a country, and this has declined from 62 percent in 2008 to 33 percent in 2012 in some of the poorest regions in Madagascar" (World Bank, 2015).

4 Modeling approach

We develop a data-driven modeling approach combining spatial modeling and discrete-event simulation to capture the dynamics of the Malagasy VSC, including the impact of the rainy season. In the remainder of this section, we first give a brief overview of the data sources (Section 4.1). We then describe our simulation model of a multi-tiered VSC (Section 4.2) including the model structure (Section 4.2.1) and the model outputs (Section 4.2.2). Next, we explain how we use spatial models to obtain critical inputs to the simulation model (Section 4.3) including the flood hazard map (Section 4.3.1), the road network and routes during the dry season (Section 4.3.2), the rainy season disruptions (Section 4.3.3), and the geographical distribution of vaccination demand to the basic health centers (Section 4.3.4). Finally, we validate our modeling approach in Section 4.4. Figure 1 provides a schematic overview of the modeling approach. We refer the reader to Appendices A, B and C for more detailed discussions of the modeling and assumptions, the data sources, and the validation.

4.1 Data sources and collaborators

The field data used in this paper is provided by UNICEF Madagascar. It comprises (i) an Effective Vaccine Management (EVM) analysis carried out in 2014, (ii) a Health System Strengthening Cash Support proposal form composed in 2014, (iii) the Health Sector Development plan for 2015-2019, proposed in 2015, (iv) an application for support from the cold chain optimisation platform from September 2016, (v) data on the district needs per vaccine antigen for the routine immunization delivery in August and September of 2015, and (vi) a file, combining 114 separate files from 2017, providing facility locations and data detailing the capacities and resources per district. In addition to providing data, UNICEF Madagascar supported us by answering data-related questions and explaining several aspects of the Malagasy VSC. Moreover, information on vaccines' representation and characteristics (e.g., number of doses required to be fully vaccinated, wastage rates), and inventory and cold chain guidelines (e.g., safety factor for order-up-to levels) are available on the WHO website.

These field data and WHO information were leveraged to estimate a substantial proportion of the model's input parameters. To obtain representative estimates for the remaining input parameters, we use a combination of spatial modeling (using open-source data), relevant literature, expert opinions, observations during field studies in SSA, and our own rationale. The

Figure 1: Schematic overview of the modeling approach

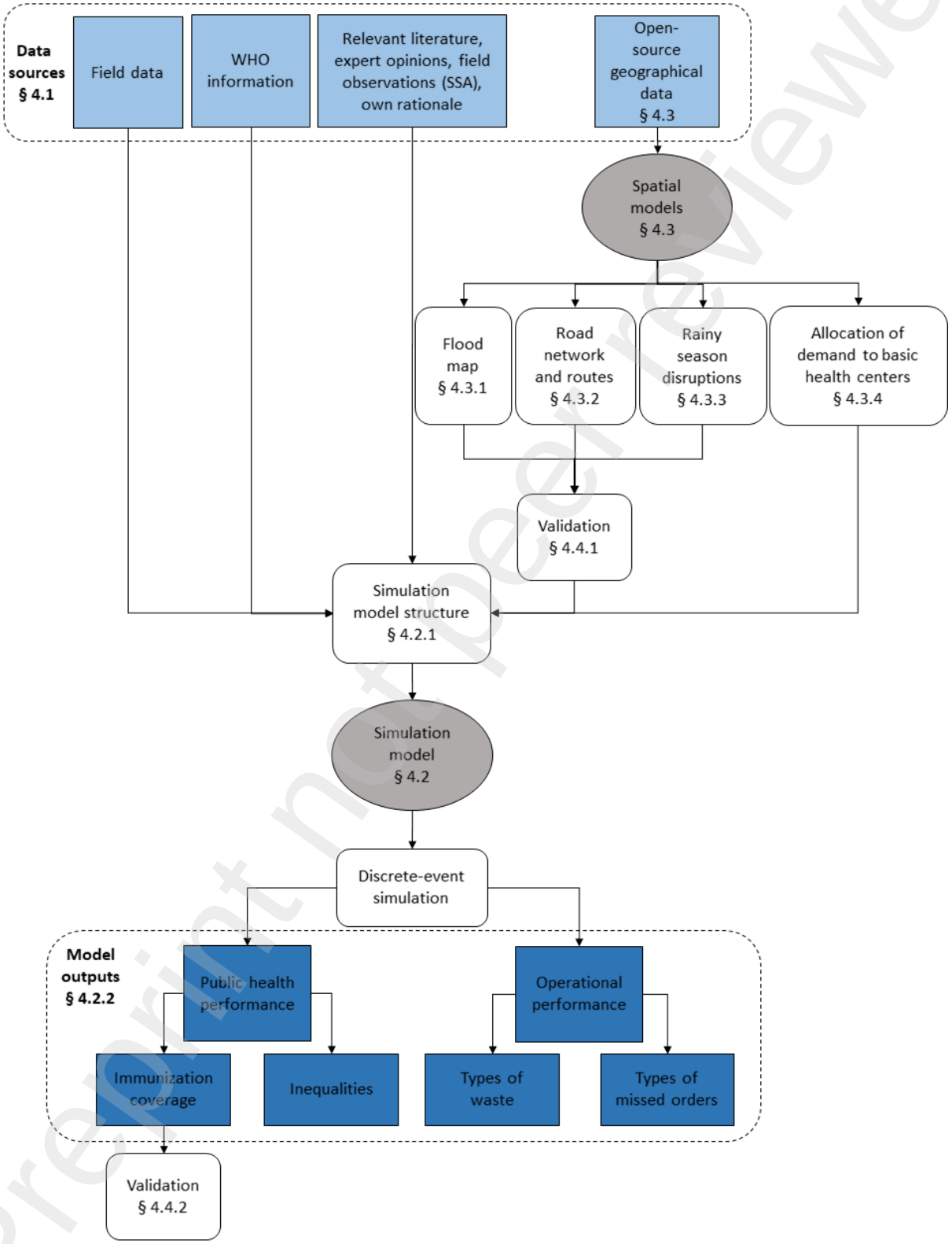

developed spatial models are explained in Section 4.3, and an overview of the model's input parameters, the type of sources used to determine the input values, and a discussion of the input values that are based on relevant literature, expert opinions, observations during field studies in SSA, and our own rationale can be found in Appendix B.

4.2 Discrete-event simulation model

Our discrete-event simulation model is designed to characterize the Malagasy childhood VSC, capturing the important characteristics and challenges inherent to a VSC in a LMIC. This means that the simulation model accounts for different types of wastage (i.e., open-vial wastage and closed-vial wastage), considers limited storage and transportation capacities, and allows for several uncertainties (i.e., unreliable storage equipment, stochastic transportation times, stochastic demand). The generic structure of our discrete-event simulation model therefore also applies to other countries in SSA.

4.2.1 Model structure

Our discrete-event model simulates the supply chain of childhood vaccines from the arrival at the national storage facility to the administration of the vaccines at the health center level. Our units of analysis are boxes containing a specified number of vaccine vials that are transported between and stored at facilities throughout the VSC. Facilities are classified as either storage facilities at the national, regional and district levels, or basic health centers at the lowest level of the supply chain. Administration of vaccines only occurs at the basic health centers. Transportation between storage facilities is conducted by one of the available transportation modes. Each vaccine antigen differs with respect to the number of doses per vial, the number of doses required to be fully vaccinated, the packed volume per vial, the wastage rate as defined by the WHO, and, for a given multi-dose vial, whether there is open-vial wastage (i.e., whether the multi-dose vial cannot be used anymore after opening).

The model is designed to capture three main aspects that cause problems in VSCs in LMICs: (i) cold chain storage bottlenecks, including CCE breakdowns and limited storage space, (ii) transportation bottlenecks, including unpredictable transportation times and limited total transportation capacity (which is a combination of the number of vehicles available, the available transportation capacity in each vehicle, and the replenishment frequency), and (iii) exogenous disruptions, i.e. the rainy season.

Table 1: Overview of main data sources used to model characteristics (more detailed overview in Appendix B)

Supply chain tier	Characteristic	Main data source
Storage facilities	Ordering process	Field data, WHO information
	Storage of vaccines	Field data, expert opinion
	Handling and execution of orders	Field data, spatial models
Basic health centers	Ordering process	Field data, WHO information
	Administration of vaccines	WHO information, spatial models

In the remainder of this subsection, we give a (high-level) overview of the model structure and highlight the most important aspects. We first discuss the main characteristics of the storage facilities at the national, regional and district levels: the ordering process of outgoing orders, the storage of vaccines (including cold chain storage bottlenecks), and the handling and execution of incoming orders at the supplying facilities (including transportation bottlenecks and rainy season disruptions). Next, we present the main characteristics of the basic health centers: the ordering process and the administration of vaccines. An overview of the main data sources used to model each of these characteristics is given in Table 1. A detailed description of the model structure, including notations, probability distributions of the stochastic parameters, and equations, is given in Appendix A.1.

Storage facilities at national, regional and district levels. The first main characteristic of the storage facilities is the ordering process of outgoing orders. The storage facilities are replenished at specified rates (usually every three months) and have an order-up-to level for each vaccine antigen.[1] When ordering vaccines, the effective storage space is taken into account. More specifically, it is possible (e.g., due to fridge breakdowns) that there is not enough storage space left at the facility to store all the planned ordered vaccines (i.e., the effective capacity is smaller than the required capacity to store the sum of all boxes of vaccines currently present at the facility and the planned ordered vaccines). In this case, the ordered quantities for each vaccine antigen are reduced proportionally to the capacity available and the volumes that were planned to be ordered. At the national level, it is possible that a replenishment is not fulfilled due to delays in the procurement process.

The second main characteristic is the storage of vaccines. Each storage facility has a number of cold rooms and fridges available. However, a significant proportion of the fridges can be

[1] In practice, the WHO often refers to this policy as the min-max policy.

obsolete. Moreover, due to the unreliability of the CCE, the limited execution of preventive maintenance, and the unavailability of spare parts, fridges fail after a stochastic life period. Depending on the type of failure, these fridges need to be repaired or replaced. Due to these cold chain failures, the effective capacity might be substantially lower than the installed capacity. In addition, when a CCE failure occurs, the resulting effective capacity might be smaller than the required capacity to store all boxes of vaccines currently present at the facility, and some boxes are therefore discarded. The number of discarded boxes for each vaccine antigen is proportional to the volumes that were stored at the facility before the CCE failure occurred. To account for local practices at many storage facilities in response to cold chain problems with respect to insufficient storage space (e.g., transporting vaccines to the nearest facility and retrieving the vaccines right before vaccination sessions), we assume that there is always at least one fridge working at each facility.

The final main characteristic is the handling and execution of incoming orders (including transportation) at the supplying facilities. This is done using fixed transportation routes. When multiple facilities are included in a transportation route, and the sum of the ordered quantities exceeds the current stock of the supplying facility, the shipped quantities are determined proportionally to the ordered quantities. Each facility has a number of transportation modes available. The transportation mode that is used to deliver the order depends both on the availability of the transportation modes and the total required capacity of all orders included in the route. First, it is checked whether a transportation mode is available that has a net capacity greater or equal to the total required capacity. Next, if no such transportation mode is currently available, the transportation mode with the greatest net capacity that is currently idle is selected. Last, if no transportation modes are currently idle, the orders are canceled. In case the net capacity of the selected transportation mode is smaller than the total required capacity, the total shipped quantities are reduced proportionally to the volumes that were planned to be shipped. After the shipped quantities are determined, the route is executed. We assume that transportation times are stochastic and drivers only depart from a facility to continue their route during working hours. During transportation, a percentage of the vaccines is lost due to e.g. breakage, depending on the transportation mode. If a facility cannot be reached due to rainy season disruptions (i.e., Section 4.3.3), it is not replenished during the rainy season. Moreover, we assume that the accessible facilities are also impacted by the rainy season, as the transportation times increase during this period of the year (in terms of average and variance).

Basic health centers. The first main characteristic of the basic health centers is the ordering process. From each basic health center, someone travels to the supplying storage facility to pick up vaccines at a specified rate. To determine the required quantities for each vaccine antigen, an order-up-to policy is applied. The order-up-to level is based on the average forecasted demand, and is increased by a wastage factor and a safety factor (i.e., 25%) as determined by the WHO.

The second characteristic is the administration of vaccines at the basic health centers, which occurs on a specified number of vaccination days per week. The demand at each basic health center for each vaccine antigen is stochastic. Moreover, the total yearly demand is capped by a maximum that is based on the basic health center's catchment area (i.e., Section 4.3.4).[2] In order to account for open-vial wastage (i.e., Section 3.1), we model the demand for each vaccine antigen in doses (instead of vials or boxes).

4.2.2 Model outputs

Each simulation replication runs for five years, of which the first two years count as the warm-up period. The model outputs are based on 50 replications. We calculate yearly statistics, thus obtaining 150 observations for each model output. We define two types of key model outputs: public health performance and operational performance. These model outputs are all related to SDG 3 that aims to increase good health and well-being for all (UN, 2019b). While the public health outcomes are directly linked to SDG 3, the operational outcomes are indirectly linked to this SDG as they provide possible explanations for, and help to define underlying causes of public health outcomes.

Public health performance. The first main public health outcome of interest is the proportion of children who have access to all required doses of all recommended vaccine antigens (by calculating the minimum vaccination coverage rate over all required vaccine antigens). We refer to this outcome as *full vaccination coverage rate*, and denote it by α. Furthermore, we report this outcome for the catchment areas of all facilities (α_{tot}), facilities that are affected by the rainy season (α_R), and facilities that are not affected by the rainy season (α_{NR}). For the remainder of the paper we refer to the latter two sets of facilities as rainy and non-rainy season affected facilities. Importantly, these full vaccination coverage rates are different from

[2]Note that this means that we include all eligible children in the demand. The rationale behind this modeled demand is that there should be a vaccine available for every child. A discussion on the demand assumption is provided in Section 6.2.

the immunization coverage rates as defined by the WHO. That is, our simulation model includes all eligible children in the demand, whereas the immunization coverage rates as defined by the WHO depend on realized demand, which is censored due to a number of influencing demand factors (e.g., operational, behavioral, social) and factors related to service delivery such as nurse availability. To understand what it takes to reach full vaccination, we look at population numbers (i.e., Section 4.3.4).[3]

The second public health outcome of the model is the mean absolute deviation in full vaccination coverage defined as

$$\text{MAD}_{fac} = \frac{\sum_j^J |\alpha_j - \alpha_{tot}|}{J}, \tag{1}$$

which provides an indication of the inequalities in full vaccination coverage between the catchment areas of the different facilities $j \in J$.

Operational performance. The first set of operational outcomes of the model are the types of waste. The model reports the maximum number of boxes wasted/discarded over the different vaccine antigens (i) because of CCE breakdown: W_{CCE}, and (ii) during transportation: W_{tr}.

The second set of operational outcomes of the model are the types of missed orders (facilities to facilities). The model reports the maximum number of missed orders (in boxes) over the different vaccine antigens because of (i) insufficient inventory at the higher level facility: MO_{inv}, (ii) unavailability of vehicles at the higher level facility: MO_{veh}, and (iii) insufficient transportation capacity: MO_{cap}.

4.3 Spatial models

A key challenge to studying geographical aspects of supply chains (including environmentally driven disruptions) is the lack of data. Similarly for our study, not all required input data could be extracted from the provided field data and WHO information (as mentioned in Section 4.1). More specifically, no detailed field data are available on the road network, the rainy season disruptions, and the geographical allocation of vaccination demand to specific basic health centers. We propose to overcome these data-related challenges and obtain realistic estimates through the use of GIS.[4] In this section, we use GIS and spatial modeling to calculate flood hazard risks

[3] Further discussion on the demand assumption is provided in Section 6.2.

[4] GIS systems are designed to capture, store, manipulate, analyze, and present geographical data. They can be used to edit data in maps, analyze and combine spatial information, and present data and outcomes of analysis.

(Section 4.3.1), to define the road network and routes during the dry season (Section 4.3.2), to predict rainy season disruptions (Section 4.3.3), and to obtain the geographical allocation of demand to the basic health centers (Section 4.3.4).

4.3.1 Flood map

To create a flood hazard map of Madagascar that identifies areas that are at high risk of flooding, we apply the method used by Kourgialas and Karatzas (2011) and Ozkan and Tarhan (2016). This method classifies each pixel[5] of the region under study into categories of flood hazard ranging from very low to very high risk by calculating a flood hazard value between 1 and 10 (where 1 and 10 indicate a very low and very high flood hazard, respectively). Similar to prior literature, we consider five factors that contribute to the flood hazard value: flow accumulation, slope, land use, rainfall intensity, and elevation (Ajin et al., 2013; Kourgialas and Karatzas, 2011; Ozkan and Tarhan, 2016). To create the final flood hazard map, we apply a linear combination of the five factor maps, using weights calculated to reflect the interaction between different factors, based on established methods (Shaban et al., 2001). We create the different factor maps using open-source data. The modeling details (including a description of how we applied the methods outlined above to Madagascar, an overview of the applied classifications, interactions and weights, and the five individual factor maps) and a description of the open-source data used can be found in Appendix A.2.1.

Applying the methods outlined above, we obtain the consolidated flood hazard map depicted in Figure 2. This map indicates that the South-East coastline and the North-Western part of Madagascar are extremely prone to flooding.

4.3.2 Road network and routes during dry season

As a map of the Malagasy road network is not available online (e.g., some routes between facilities could not be found using OpenStreetMap), we define it using established spatial modeling approaches. For this purpose, we use the friction surface expressed as the maximum rates at which humans can move through each pixel of the world's surface (expressed in minutes per meter). These open-source data are obtained from the project on accessibilities to cities of the Malaria Atlas Project (Earth Engine Data Catalog, 2019; Weiss et al., 2018). The inputs used to create this friction surface map consist of gridded surfaces that quantify the geograph-

[5] A pixel is the unit of analysis for spatial models, proportional in size to the resolution of the underlying map.

Figure 2: Flood hazard map

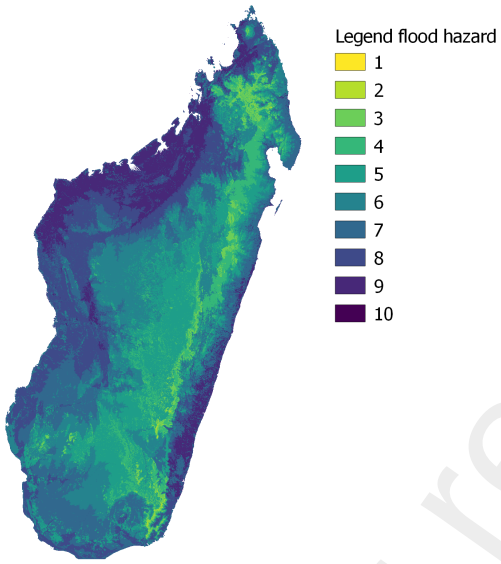

ical positions and salient attributes of roads, railways, rivers, water bodies, land cover types, topographical conditions (slope angle and elevation), and national borders (Weiss et al., 2018).

We approximate the Malagasy road network during the dry season by removing pixels in the friction surface map that correspond to speeds below 10 kilometers per hour (as the speed to travel by foot or river boat is below 10 kilometers per hour). In this way, we obtain the road network shown in Figure 3a.[6] To calculate the transportation times between facilities, we locate the facilities on the road map and define the routes between the facilities using GIS.

4.3.3 Rainy season disruptions

To define the road network during the rainy season, we combine the flood hazard map (Section 4.3.1) with the map of the road network during the dry season (Section 4.3.2). That is, we determine a threshold on the flood hazard value above which a pixel of the map is considered flooded. In this study, we consider areas with a flood hazard value of 7.5 or higher as flooded. This threshold value corresponds to a high flood hazard risk according to the classifications of Kourgialas and Karatzas (2011) and Ozkan and Tarhan (2016), and the corresponding flooded areas include the areas indicated by field data. The flooded pixels are removed from the road network during the dry season in order to obtain the road network during the rainy season (depicted in Figure 3b).

[6]Note that we converted the speeds from minutes per meter to minutes per kilometer for the sake of clarity.

Figure 3: The Malagasy road network during (a) the dry season and (b) the rainy season

(a) Dry season

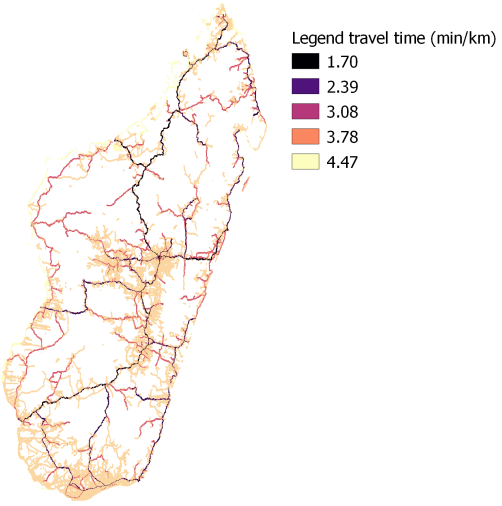

(b) Rainy season

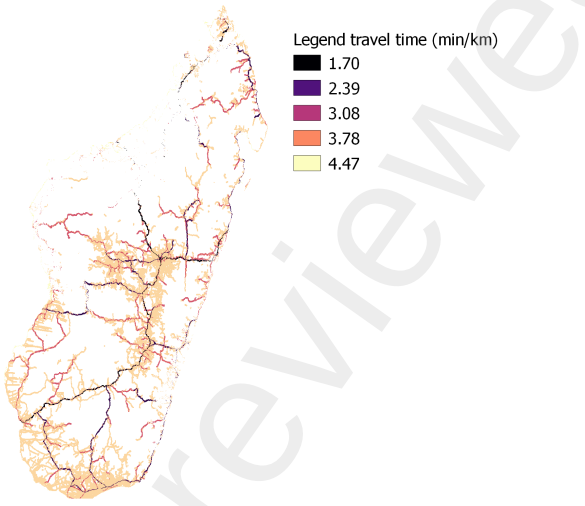

To determine the facilities that are affected during the rainy season (i.e., facilities that are cut off from the road network), we define the routes between the facilities using the road map during the rainy season shown in Figure 3b. If no route from the supplying facility to a facility exists, the latter is considered to be rainy season affected. We predict that 39% of facilities are impacted by the rainy season with respect to disrupted roads. Figure 8 in Appendix A.2.2 gives a geographical overview of these facilities.

4.3.4 Geographical allocation of demand to the basic health centers

To define the catchment areas of the basic health centers, we use the friction surface explained in Section 4.3.2 (Earth Engine Data Catalog, 2019; Weiss et al., 2018) and the locations of the basic health centers (Madagascar Decision Support System, 2019). We furthermore assume that people will go to the basic health center that they can reach the fastest (i.e., they minimize their traveling time). Combining this information using spatial modeling, we obtain the catchment areas of the basic health centers and the corresponding travel times (during the dry season) to the nearest health center (depicted in Figure 9 in Appendix A.2.3).

To obtain the number of children that need to be vaccinated in each basic health center's catchment area, we use estimates of the number of births per pixel. These open-source data are obtained from Worldpop (Worldpop, 2019) and contain numbers of live births with national totals adjusted to match UN national estimates. These data are produced by integrating multiple data sources on population distribution, age structure, and fertility rates. Further details

on the methods used to create these data can be found in James et al. (2018) and Tatem et al. (2014). Combining the numbers of live births with the catchment areas of the basic health centers using spatial modeling, we obtain estimates of the number of children that need to be vaccinated in each basic health center's catchment area.

4.4 Model validation

4.4.1 Spatial models

As the construction of the spatial maps is motivated by the absence of detailed data, it is not possible to validate the maps on the basis of field data. We therefore validate the obtained flood hazard and road map by comparing our outcomes with publicly available information.

First, a categorized flood hazard map (in the form of an image), indicating flood risks in Madagascar, is made available by OasisHub, a research program that publishes environmental data (OasisHub, 2019; Climate-ADAPT, 2019). The areas and degrees of risk indicated on the map provided by OasisHub are similar (by visual inspection) to those identified on the flood hazard map that we constructed in Section 4.3.1 (i.e., Figure 10 in Appendix C).

Second, an overview of the Malagasy road network is obtained from the Logistics Capacity Assessment (LCA) tool, a tool hosted by the World Food Program (LCA, 2019a,b). LCAs give an overview of the logistics infrastructure, processes and regulations, markets, and contacts in over 100 countries. The road infrastructure provided by the LCA matches (by visual inspection) the road network during the dry season that we developed in Section 4.3.2 (i.e., Figure 11 in Appendix C). Also, the routes between facilities that can be found via OpenStreetMap and GoogleMaps are similar to the ones found using our map of the road network.

Finally, our flood hazard map (Figure 2) and the road maps during the dry and rainy season (Figure 3) were validated through collaborator discussions.

4.4.2 Simulation model

Validating the outcomes of the simulation model poses a challenge for various reasons. First of all, the only performance measures that are publicly available are the immunization coverage rates as defined by the WHO. These can be accessed through the WHO website (WHO/UNICEF, 2018) or through the website of the Demographic and Health Surveys (DHS) (Demographic and Health Surveys Program, 2019). As mentioned in Section 4.2, these immunization coverage

Table 2: Comparison of reported immunization coverage rates and simulated full vaccination coverage rates

Level of aggregation	Region	WHO data (2014)	DHS data (2008-2009)	Simulation output α_{tot} (2014)
National	Madagascar	64.00	61.60	61.63
Regional	Alaotra Mangoro	-	B	B
	Amoron'i Mania	-	B	B
	Analamanga	-	B	B
	Analanjirofo	-	B	W
	Androy	-	W	W
	Anosy	-	W	B
	Atsimo Andrefana	-	W	B
	Atsimo Atsinanana	-	W	W
	Atsinanana	-	B	W
	Betsiboka	-	W	W
	Boeny	-	W	W
	Bongolava	-	B	B
	Diana	-	B	B
	Haute Matsiatra	-	B	B
	Ihorombe	-	W	W
	Itasy	-	B	B
	Melaky	-	W	B
	Menabe	-	W	B
	Sava	-	W	W
	Sofia	-	W	W
	Vakinankaratra	-	B	B
	Vatovavy Fitovinany	-	W	W

Notes: B: better than national performance, W: worse than national performance.

rates are based on the realized demand (and are therefore censored as they are affected by stock-outs, nurse availability, and a number of influencing operational, behavioral and social factors), whereas the full vaccination coverage rates from the simulation model are based on population numbers to understand what it takes to get full immunization. Second, these data are mostly only available at the national level. Only the DHS data is disaggregated and provides immunization coverage rates at both national and regional levels. However, the most recent DHS data on immunization coverage rates in Madagascar dates from 2008-2009. Therefore, an exact comparison between the immunization coverage rates available on the WHO and DHS websites, and the full vaccination coverage rates from the simulation model is not possible.

Although an exact comparison is not meaningful, we make an attempt to validate the simulation model by (i) comparing the national full vaccination coverage from the simulation model α_{tot} with national immunization coverage rates recorded in WHO and DHS data (WHO/UNICEF, 2018; Demographic and Health Surveys Program, 2019), and (ii) comparing the regions in terms of 'better than national: B' or 'worse than national: W' performance. From the DHS data, we use the variable 'received all 8 basic vaccinations' from the 2008-2009 survey.

Table 2 indicates that our simulation model correctly predicts the national full vaccination

coverage, and that it captures the differences between regions. That is, the model correctly predicts whether a region performs better or worse than the national coverage rate for 73% of the regions. Moreover, since our modeling approach focuses on the supply of vaccines, modeling the rainy season and operational decisions, but does not include behavioral or social demand aspects, it indicates which regions are performing below average due to supply issues. Therefore, the results in Table 2 suggest that 67% (8 out of the 12 regions labeled as 'W' in the DHS data) of regions with low reported immunization coverage rates are affected by operational inefficiencies or rainy season disruptions. The observed differences between the DHS data and the simulation outcomes might be explained by (i) demand for vaccinations that is substantially lower than the maximum demand in poor or remote areas, (ii) immunization rates that are close to the national immunization coverage rate, or (iii) differences between 2008-2009 and 2014.

Overall, we believe that the results in Table 2 suggest that our modeling approach, combining spatial modeling and discrete-event simulation, satisfactorily captures the behavior of the Malagasy VSC.

5 Results and policy insights

In this section, we first report simulated estimates of the model outputs for the baseline scenario (Section 5.1). Next, based on these results, we study the effect of several shorter-term modifications to the current Malagasy VSC (Section 5.2). Last, we illustrate how our modeling approach can be applied to assess the impact of an increase in flooding due to climate change (Section 5.3).

5.1 Baseline scenario and effect of rainy season

First, consider the simulated model outputs of the baseline scenario which approximates the stochastic behavior of the current Malagasy VSC (depicted in Table 3).

Observation 1. Substantial inequalities in full vaccination coverage between rainy and non-rainy season affected facilities, and between facilities in general, are present in the current Malagasy VSC. An estimated gap of 27 percentage points exists between rainy and non-rainy season affected facilities, while our measure of inequality, MAD_{fac}, equals 25%.

Whereas the national full vaccination coverage α_{tot} equals 62%, there is a substantial difference between the vaccination coverage of rainy season affected facilities α_R which equals 43%

Table 3: Simulation outputs of the current Malagasy VSC

	Mean	95% CI
Public health performance		
α_{tot} (%)	62	[61; 62]
α_R (%)	43	[43; 43]
α_{NR} (%)	70	[70; 70]
MAD_{fac} (%)	25	[25; 25]
Operational performance		
W_{CCE} (boxes)	373	[329; 416]
W_{tr} (boxes)	1682	[1617; 1693]
MO_{inv} (boxes)	22292	[21812; 22771]
MO_{veh} (boxes)	162	[79; 245]
MO_{cap} (boxes)	29745	[29320; 30171]

Notes: α_{tot}, α_R, α_{NR}: full vaccination coverage based on all facilities, the rainy season affected facilities, and the non-rainy season affected facilities, respectively. MAD_{fac}: mean absolute deviation. W_{CCE}, W_{tr}: waste due to CCE breakdowns and during transportation, respectively. MO_{inv}, MO_{veh}, MO_{cap}: missed orders due to insufficient inventory, unavailable vehicles, and insufficient vehicle capacity, respectively.

and that of non-rainy season affected facilities α_{NR} which equals 70%. This results in a gap of 27 percentage points, meaning that the burden of vaccine preventable diseases falls disproportionally on the rainy season affected areas. Moreover, in line with prior literature, we find that there are important inequalities (a simulated mean of 25% for MAD_{fac}) in full vaccination coverage between facilities in general in Madagascar (van den Ent et al., 2017).

Observation 2. In the current Malagasy VSC, missed orders (52,199 boxes annually or 96% of the sum of missed orders and discarded boxes) are a larger source of operational inefficiency than wasted vials (2,055 boxes annually or 4% of the sum of missed orders and discarded boxes). Most of these missed orders are due to either insufficient inventory (22,292 boxes or 42.5% of the missed orders) or insufficient vehicle capacity (29,745 boxes or 57% of the missed orders).

The operational mechanisms driving the health outcomes can also be observed in Table 3. The results indicate that in the baseline scenario, a substantial number of missed orders is due to insufficient inventory or vehicle capacity. That is, whereas only 0.5% of missed orders is due to the unavailability of vehicles, 42.5% and 57% of missed orders are induced by insufficient inventory at the higher level facility and insufficient vehicle capacity, respectively. The outputs in Table 3 also show that the total number of discarded boxes is mainly driven by issues during transportation (82% of discarded boxes), and to a limited extent by CCE breakdowns (18% of discarded boxes). Consequently, it seems that the major operational issues in the

current Malagasy VSC are the missed orders due to insufficient inventory and vehicle capacity. Moreover, given the limited number of discarded boxes due to CCE breakdowns, the missed orders due to insufficient inventory are not because inventory at the facility is being discarded, but because the boxes never got there as the facility was not replenished by the upper level facility as it should have been. This also explains the relatively low number of wasted boxes as boxes cannot be discarded if they do not reach the facility.

Observation 3. The main drivers for the public health performance of the current Malagasy VSC are:

(i) Rainy season disruptions: Substantial inequalities are observed between rainy and non-rainy season affected facilities.

(ii) Operational inefficiencies: The vehicle capacity constitutes an operational bottleneck, impeding the flow of vaccines through the network.

Based on these simulated public health and operational outcomes, we identify two main drivers that explain the observed low vaccination coverage and high inequalities. On the one hand, the presence of the rainy season introduces an inequality gap between rainy and non-rainy season affected facilities as the former are not replenished throughout the rainy season. On the other hand, a shortage in vehicle capacity impedes the flow of vaccines through the VSC, resulting in insufficient inventory at the facilities (in both the rainy and non-rainy season).

5.2 Effect of modifications to the Malagasy vaccine supply chain

Based on Observation 3, we consider the impact of two types of shorter-term modifications to the Malagasy VSC: (i) introducing a rainy season inventory buffer for the rainy-season affected facilities, and (ii) increasing the replenishment frequency. Both of these modifications have been discussed by UNICEF Madagascar.

The first modification aims at mitigating the effect of the first driver, i.e. the rainy season disruptions. Introducing a rainy season inventory buffer should increase the inventory levels at the rainy season affected facilities, thereby reducing the number of stock-outs due to canceled shipments during the rainy season. These rainy season buffers are implemented by increasing the order-up-to levels (which already include a safety stock as determined by the WHO) of the rainy season affected facilities. More specifically, in this study, we increase the order-up-to levels with 50% and 100%, respectively. Note that a 100% buffer covers the entire demand during the

Table 4: Simulation outputs of the current Malagasy VSC and the impact of the considered modifications

Replenishment frequency	1 month			2 months			3 months		
Rainy season buffer	No buffer	50%	100%	No buffer	50%	100%	No buffer	50%	100%
Public health performance									
α_{tot} (%)	80	83	85	75	77	79	62	62	63
α_R (%)	58	67	72	54	59	63	43	46	46
α_{NR} (%)	90	90	91	85	85	86	70	70	70
MAD_{fac} (%)	17	13	11	21	19	20	25	26	27
Operational performance									
W_{CCE} (boxes)	61	88	174	301	433	510	373	429	383
W_{tr} (boxes)	2295	2412	2490	2127	2209	2243	1682	1694	1703
MO_{inv} (boxes)	15503	15752	16758	16578	20514	26782	22292	30397	39108
MO_{veh} (boxes)	10559	11324	11799	1445	1487	1062	162	233	254
MO_{cap} (boxes)	1680	2540	4021	9154	14491	19277	29745	35893	39451

Notes: α_{tot}, α_R, α_{NR}: full vaccination coverage based on all facilities, the rainy season affected facilities, and the non-rainy season affected facilities, respectively. MAD_{fac}: mean absolute deviation. W_{CCE}, W_{tr}: waste due to CCE breakdowns and during transportation, respectively. MO_{inv}, MO_{veh}, MO_{cap}: missed orders due to insufficient inventory, unavailable vehicles, and insufficient vehicle capacity, respectively.

rainy season. However, due to limited storage space, it is possible that a facility does not have enough storage space left to store the required buffer. In that case, the order-up-to levels are increased until the maximum storage space is reached.

The second modification aims at reducing the impact of the second driver, i.e. the vehicle capacity bottleneck. There are two obvious ways to do this: (i) increasing the vehicle capacity (e.g., buying vehicles with larger capacity), or (ii) increasing the replenishment frequency, thereby reducing the quantities that need to be transported during a single shipment. In this study, we investigate the effect of increasing the replenishment frequency, since this is a shorter-term modification that can be realized with minimal efforts and resources. More specifically, we increase the replenishment frequency from every third month to every second month and every month, respectively. Table 4 reports the simulated outcomes of these experiments. A more detailed overview of these outcomes (including the 95% confidence intervals) can be found in Appendix D.

Observation 4. To achieve the full mitigation potential of the rainy season buffer, operational bottlenecks must be concurrently addressed (see Figure 4). By increasing the replenishment frequency from trimestral to monthly shipments, the impact of implementing a 100% rainy season buffer on vaccination coverage rates α_{tot} and α_R increases from 1 to 5 percentage points, and from 3 to 14 percentage points, respectively.

First, consider the impact of only implementing a rainy season buffer (while maintaining trimestral shipments). Table 4 and Figure 4 show that solely increasing the order-up-to levels of the rainy season affected facilities with 100% only slightly (although statistically significant according to the 95% confidence intervals in Appendix D) improves α_{tot} with 1 percentage point. This improvement is entirely attributed to the rainy season affected facilities as α_R increases with 3 percentage points, resulting in a decrease of the gap between α_{NR} and α_R of 3 percentage points. Although resulting in an improvement of public health performance, the estimated impact is limited. This is due to the substantial increase in the estimated number of missed orders due to insufficient inventory MO_{inv} and insufficient vehicle capacity MO_{cap}. These results imply that the observed limited effect of implementing a rainy season buffer is due to operational inefficiencies hampering the flow of vaccines through the network. This, in turn, impedes the rainy season affected facilities from actually reaching the order-up-to levels, thereby not realizing the full potential benefits of implementing a rainy season buffer.

To further investigate this issue, Figure 5 gives an overview of the estimated total number of delivered boxes during one year for each vaccine antigen at the district level for different scenarios. In order to get insights into the differing impact on rainy and non-rainy season affected facilities, these outcomes are calculated separately for (i) all district facilities, (ii) only the rainy season affected district facilities, and (iii) only the non-rainy season affected facilities. Figure 5 confirms our observation that the flow of vaccines through the network is blocked, as solely implementing a 100% rainy season buffer does not substantially increase the number of delivered boxes at the district level.

Next, we look at the effect of only increasing the replenishment frequency (without implementing a rainy season buffer). Solely altering the replenishment frequency from trimestral to monthly shipments considerably improves α_{tot} with 18 percentage points. We also note the substantial increase in the number of delivered boxes depicted in Figure 5. This again confirms the vehicle capacity bottleneck in the current network. However, the results in Table 4 and Figure 4 also show that increasing the replenishment frequency is predicted to widen the inequality gap between rainy and non-rainy season affected facilities: the difference between α_{NR} and α_R increases with 5 percentage points. This can be explained by the two drivers defined in observation 3. Whereas rainy season disruptions only affect the rainy season affected facilities, operational inefficiencies have an impact on all facilities. If the operational inefficiencies are mostly resolved (i.e., by increasing the replenishment frequency), then the only driver left

Figure 4: Full vaccination coverage rates

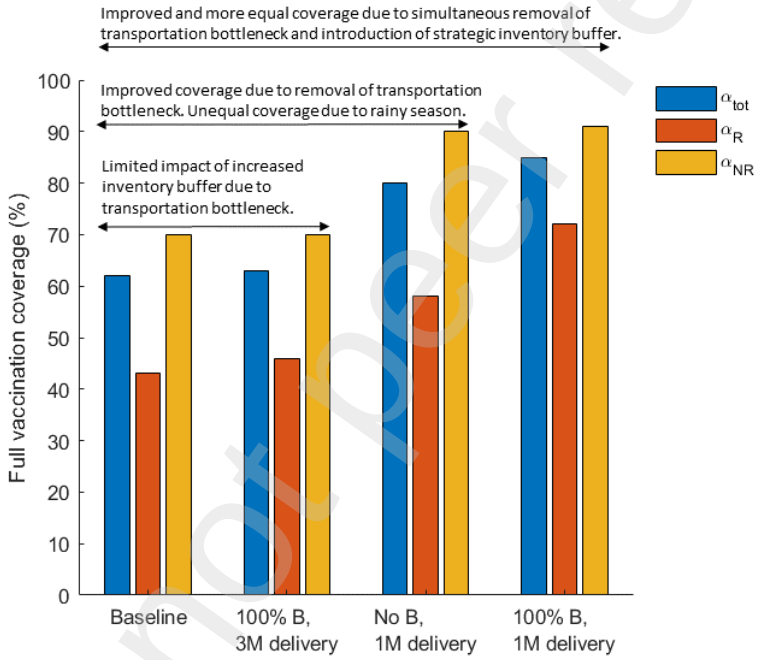

Notes: The four scenarios depicted are (i) Baseline scenario (no rainy season buffer, trimestral shipments), (ii) 100% B, 3M delivery (100% rainy season buffer, trimestral shipments), (iii) No B, 1M delivery (No rainy season buffer, monthly shipments), and (iv) 100% B, 1M delivery (100% rainy season buffer, monthly shipments).

Figure 5: Total number of delivered boxes at district level

(a) All district facilities

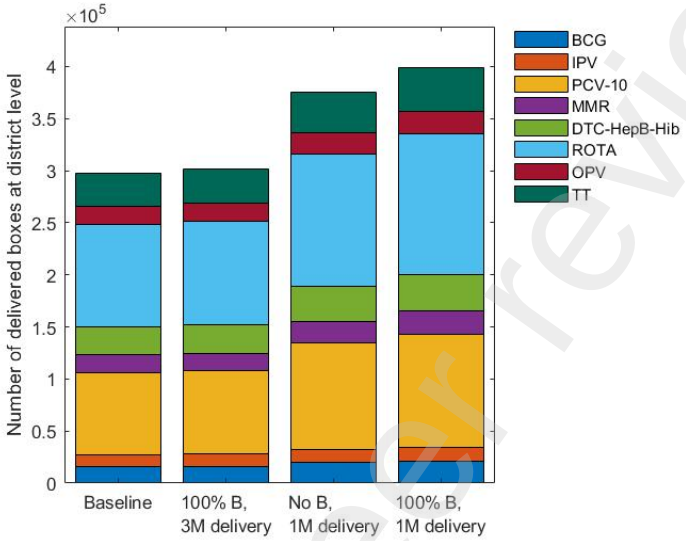

(b) Rainy season affected district facilities

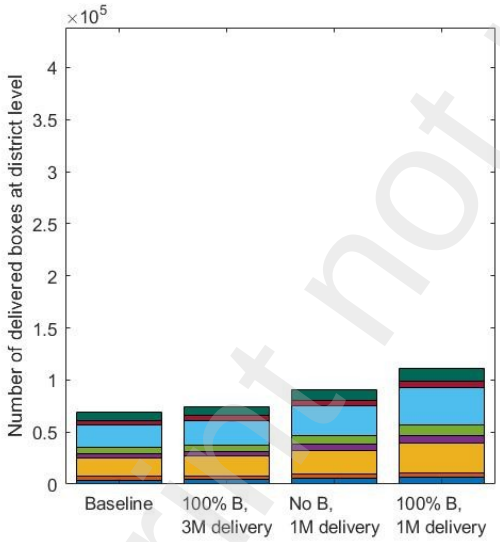

(c) Non-rainy season affected district facilities

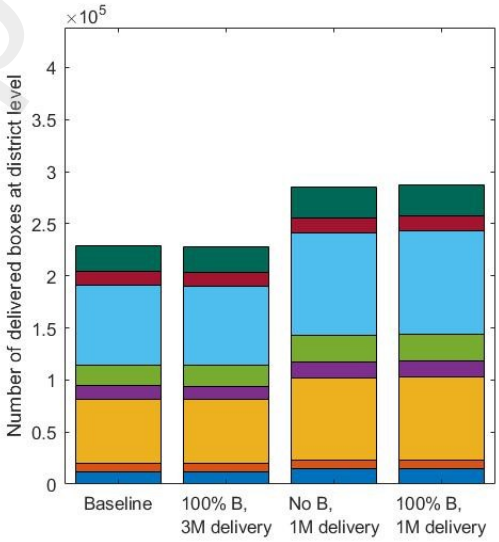

Notes: Average simulated total number of delivered boxes at the district level calculated separately for (a) all district facilities, (b) only rainy season affected district facilities, and (c) only non-rainy season affected district facilities. The four scenarios depicted in each subfigure are (i) Baseline scenario (no rainy season buffer, trimestral shipments), (ii) 100% B, 3M delivery (100% rainy season buffer, trimestral shipments), (iii) No B, 1M delivery (No rainy season buffer, monthly shipments), and (iv) 100% B, 1M delivery (100% rainy season buffer, monthly shipments).

hampering the public health performance of the VSC is the rainy season. This then results in higher inequalities between rainy and non-rainy season affected facilities.

Last, consider both modifications simultaneously. That is, we implement a 100% rainy season buffer while introducing monthly shipments. Table 4 and Figure 4 show that this results in a substantial improvement of the public health outcomes compared to the baseline scenario. The estimated national full vaccination coverage α_{tot} increases with 23 percentage points (from 62% to 85%). This means an estimated 38% increase in the number of children that can be reached with all basic vaccinations. While the vaccination coverage rates of both the rainy and non-rainy season affected facilities show a considerable improvement, the rainy season affected facilities benefit the most with an increase of 29 and 21 percentage points in full vaccination coverage for the rainy and non-rainy season affected facilities, respectively. This, in turn, reduces the inequality gap between rainy and non-rainy season affected facilities: the difference between α_{NR} and α_R decreases from an estimate of 27 percentage points to 19 percentage points. Moreover, a considerable reduction in the inequality gap between facilities in general can be observed: MAD_{fac} decreases from an estimate of 25% to 11%.

Also note the impact of combining these two modifications compared to solely increasing the rainy season buffer or only altering the replenishment frequency. First, adding monthly replenishment frequencies to a 100% rainy season buffer enables to realize the impact of implementing this buffer as the operational bottleneck is now relieved. This is also demonstrated in Figure 5 by the increase in total delivered boxes at the district level. Second, implementing a 100% rainy season buffer on top of monthly shipments further improves α_{tot} (compared to solely introducing monthly shipments) by 5 percentage points. Moreover, this improvement is mainly attributed to the rainy season affected facilities with a substantial improvement of α_R of 14 percentage points. This shows that the rainy season has an important impact on health performance and that implementing a rainy season buffer can significantly mitigate this impact, if there are no substantial operational inefficiencies hampering the flow of vaccines through the VSC network.

These results have implications for policy and practice. The substantial estimated improvements in health outcomes show that implementing shorter-term modifications such as increasing the replenishment frequency and implementing an additional rainy season buffer can significantly impact the performance of the VSC. It therefore seems important to first investigate and focus on these or similar shorter-term modifications, before concentrating on longer-term interven-

tions (e.g., adding CCE, buying new vehicles with larger capacities) as the latter are typically more expensive, take more time and effort to be implemented, and might involve higher risks. This is especially relevant as resources are limited in these VSC settings. Moreover, it seems important to also investigate the presence of operational inefficiencies and to study modifications that reduce those inefficiencies, as potential improvements in public health performance (e.g., implementing a rainy season buffer to mitigate the impact of the rainy season) might be hampered by operational inefficiencies.

Observation 5. A trade-off might exist between full vaccination coverage rates (or other health performance indicators) and equity measures. Whereas introducing monthly shipments and a 100% rainy season buffer improves all public health indicators, only increasing the replenishment frequency while not implementing any rainy season buffer improves national vaccination coverage at the cost of a widening inequality gap between rainy and non-rainy season affected facilities compared to the baseline scenario.

The results shown in Table 4 and Figure 4 also indicate that a trade-off might be present between full vaccination coverage rates on the one hand and equity measures on the other hand. One example was already discussed above where introducing monthly replenishment frequencies increases α_{tot}, but also widens the inequality gap between α_{NR} and α_R. In addition, consider the case where we do not introduce a rainy season buffer and increase the replenishment frequency from every 3 months to every 2 months. This modification results in a substantial increase of α_{tot}, α_R, and α_{NR} of 13, 11, and 15 percentage points, respectively. However, it also leads to a widening inequality gap between rainy and non-rainy season facilities as the difference between α_{NR} and α_R increases from 27 percentage points to 31 percentage points. These outcomes suggest that, in this case, the overall improvement is disproportionally allocated to the non-rainy season affected facilities. Therefore, other modifications might be preferred.

This result is important from a policy perspective because it underscores the importance of considering equity measures. In addition, it avoids scenarios where an overall improvement is, unwillingly, accompanied by a widening inequality gap. This is also relevant as international health and humanitarian organizations are increasingly emphasizing and advocating for equitable access to healthcare.

5.3 Impact of an increase in flooding due to climate change

SDG 13 pleads to "take urgent action to combat climate change and its impacts" (UN, 2019a). Improving the climate resiliency of the Malagasy VSC is necessary as sea levels will rise in the future due to climate change, increasing the number of transportation links and facilities affected by the rainy season (USAID, 2017). In addition, the World Bank states that "Madagascar is one of the African countries most severely affected by climate change impacts" and has recently (i.e., December 2019) approved a $50 million grant to increase Madagascar's disaster and climate resiliency (World Bank, 2019a,b).

In this section, we illustrate how our modeling approach can be applied to assess the impact of an increase in flooding due to climate change. Unfortunately, to the best of our knowledge, no detailed information is currently available about the magnitude of the expected future increase in rainy season affected facilities. As explained in Section 4.3.3, we use a threshold value of 7.5 to determine the flooded areas in the baseline scenario. This threshold value corresponds to a high flood hazard risk according to the classifications of Kourgialas and Karatzas (2011) and Ozkan and Tarhan (2016), and the corresponding flooded areas include the areas indicated by field data. To illustrate the potential impact of climate change on the Malagasy VSC, we decrease the threshold value above which a pixel of the road network is considered to be flooded from 7.5 to 7. We choose this value because a flood hazard value of 7 still corresponds to a relatively high risk (i.e., according to Kourgialas and Karatzas (2011) and Ozkan and Tarhan (2016), a flood hazard value between 5 and 8 corresponds to a moderate to high risk), while a decrease of 0.5 is not too extreme. This relatively small decrease in flood hazard threshold value results in a substantial 37% increase in the number of rainy season affected facilities.

We first look at the impact of an increase in flooding on the current Malagasy VSC operations (i.e., trimestral shipments and no additional rainy season buffer). A comparison between the simulated outcomes of the baseline scenario and the considered increase in rainy season affected facilities is given in Table 5.

Observation 6. In the absence of policy action to make the VSC more robust, even a moderate increase in flooding will result in a significant 37% increase in facilities being affected by the rainy season and, in turn, have an impact on the public health performance of the Malagasy VSC by (i) decreasing the number of fully vaccinated children by 4%, and (ii) further widening the inequality gap between rainy and non-rainy season affected facilities with 3 percentage points.

Table 5: Simulation outputs of the impact of a 37% increase in rainy season affected facilities on the baseline scenario

	Baseline		Climate change		Impact
	Mean	95% CI	Mean	95% CI	
Public health performance					
α_{tot} (%)	62	[61; 62]	59	[59; 59]	-3
α_R (%)	43	[43; 43]	42	[41; 42]	-1
α_{NR} (%)	70	[70; 70]	72	[71; 72]	+2
MAD_{fac} (%)	25	[25; 25]	25	[25; 25]	Not significant
Operational performance					
W_{CCE} (boxes)	373	[329; 416]	373	[331; 415]	Not significant
W_{tr} (boxes)	1682	[1617; 1693]	1589	[1579; 1600]	-93
MO_{inv} (boxes)	22292	[21812; 22771]	19702	[19238; 20165]	-2590
MO_{veh} (boxes)	162	[79; 245]	199	[104; 294]	Not significant
MO_{cap} (boxes)	29745	[29320; 30171]	26631	[26264; 26997]	-3114

Notes: α_{tot}, α_R, α_{NR}: full vaccination coverage based on all facilities, the rainy season affected facilities, and the non-rainy season affected facilities, respectively. MAD_{fac}: mean absolute deviation. W_{CCE}, W_{tr}: waste due to CCE breakdowns and during transportation, respectively. MO_{inv}, MO_{veh}, MO_{cap}: missed orders due to insufficient inventory, unavailable vehicles, and insufficient vehicle capacity, respectively.

A mild increase in flooding due to climate change (by decreasing the flood hazard threshold value with 0.5), is estimated to reduce the national full vaccination coverage α_{tot} with 3 percentage points (from 62% to 59%). This decrease in national vaccination coverage results in an estimated 4% reduction in fully vaccinated children. Moreover, the rainy season affected facilities bear the largest burden of this deterioration. Whereas the estimated full vaccination coverage of the non-rainy season affected facilities α_{NR} increases from 70% to 72%, that of the rainy season affected facilities decreases from 43% to 42%. (Note that the increase of α_{NR} can be explained by higher inventory levels at non-rainy season affected upper level facilities as rainy season affected lower level facilities are not supplied during the rainy season.) This results in a widening of the inequality gap between rainy and non-rainy season affected facilities: the simulated difference between α_{NR} and α_R increases with 3 percentage points (from 27 percentage points to 30 percentage points).

These results are important from a policy perspective because they indicate that in the absence of policy action, even a mild increase in flooding due to climate change can have an important impact on the public health performance of the Malagasy VSC by (i) decreasing the national full vaccination coverage and thus the number of fully vaccinated children, and (ii) further widening the vaccination inequality gap between rainy and non-rainy season affected facilities. These outcomes thus underscore the importance of increasing the climate resiliency

Table 6: Simulation outputs of an increase in the number of rainy season affected facilities and the impact of the modifications

Replenishment frequency	1 month			2 months			3 months		
Rainy season buffer	No buffer	50%	100%	No buffer	50%	100%	No buffer	50%	100%
Public health performance									
α_{tot} (%)	76	81	83	72	73	75	59	60	60
α_R (%)	58	67	71	53	58	61	42	43	44
α_{NR} (%)	90	91	91	85	85	85	72	72	71
MAD_{fac} (%)	19	14	12	22	21	23	25	27	28
Operational performance									
W_{CCE} (boxes)	63	173	243	313	449	463	373	380	396
W_{tr} (boxes)	2139	2324	2401	1996	2060	2096	1589	1604	1609
MO_{inv} (boxes)	15314	14717	20544	15191	23615	32442	19702	31677	43019
MO_{veh} (boxes)	8694	9462	9922	1289	1213	1379	199	214	201
MO_{cap} (boxes)	1656	2854	5053	8446	16376	22704	26631	34307	39431

Notes: α_{tot}, α_R, α_{NR}: full vaccination coverage based on all facilities, the rainy season affected facilities, and the non-rainy season affected facilities, respectively. MAD_{fac}: mean absolute deviation. W_{CCE}, W_{tr}: waste due to CCE breakdowns and during transportation, respectively. MO_{inv}, MO_{veh}, MO_{cap}: missed orders due to insufficient inventory, unavailable vehicles, and insufficient vehicle capacity, respectively.

of the Malagasy VSC.

We next consider the impact of an increase in flooding on the different shorter-term modifications introduced in Section 5.2. The simulated outcomes for all combinations of rainy season buffers and replenishment frequencies when an increase in the number of rainy season affected facilities occurs are shown in Table 6. A more detailed overview of these outcomes (including the 95% confidence intervals) is given in Appendix D.

Observation 7. Additional actions are needed to increase the climate change resiliency of the Malagasy VSC. Although introducing monthly shipments and implementing a 100% rainy season buffer mitigates the impact of increased flooding due to climate change compared to the baseline scenario, it cannot prevent a 3% deterioration in fully vaccinated children.

The results in Table 6 indicate that introducing monthly shipments and a 100% rainy season buffer remains the best scenario (based on public health outcomes) as it maximizes the national full vaccination coverage α_{tot} while minimizing the inequality gaps. Moreover, comparing the results in Table 4 and Table 6 demonstrates that the estimated impact of increased flooding due to climate change in this scenario is less severe than in the baseline scenario.

Nevertheless, comparing the results in Table 4 and Table 6 also shows that none of the scenarios is sufficiently resilient to protect the Malagasy VSC against the considered consequences of climate change. The national full vaccination coverage α_{tot} in the best scenario decreases

with 2 percentage points, resulting in a 3% decrease in fully vaccinated children. Although the inequality gap between rainy and non-rainy season affected facilities is not substantially impacted, the overall vaccination inequality gap widens: MAD_{fac} increases from 11% to 12%.

Based on these results, it seems necessary to investigate additional longer-term actions. Such actions might include installing additional CCE at rainy season affected facilities, changing (part of) the transportation links during the rainy season, relocating facilities, and adding transportation modes that are better able to deal with flooded or extremely muddy roads (e.g., 4x4 trucks, drones).

6 Conclusion

6.1 Summary of main insights

In several LMICs, the already challenging task of getting the required vaccines to the targeted population is further complicated by the presence of a rainy season. To the best of our knowledge, this paper is the first to study the impact of the rainy season on the public health performance of VSCs in LMICs. Using the context of the Malagasy VSC, we assess the impact of the rainy season on vaccination coverage rates and inequalities, and we investigate various mitigation strategies. Our findings provide contextual information and insights that are relevant for policy and practice. Also, our results contribute to achieving the UNSDGs by providing actionable insights for improving vaccination coverage (SDG 3) and investigating the resiliency of the VSC to increased flooding due to climate change (SDG 13).

To do so, we develop a data-driven modeling approach combining spatial modeling and discrete-event simulation. GIS and spatial modeling prove to be promising methodologies to face data-related challenges. More specifically, we use spatial modeling to predict realistic estimates for the road network, the parts of the supply chain network that are likely to be disrupted during the rainy season, and the geographical distribution of demand. The use of GIS and spatial modeling therefore provides an opportunity for the operations management community, and the humanitarian and global/public health operations community in particular as the latter operate in settings where data-related challenges are abundantly present. For example, GIS and spatial modeling might be used to estimate the road network, or to predict regions and roads that are vulnerable to geographical problems (e.g., rain, snow, droughts) or disasters (e.g., hurricanes, landslides). Our discrete-event simulation model characterizes the

supply chain of childhood vaccines in LMICs, thereby capturing the important characteristics and challenges inherent to these settings (i.e., different types of wastage, limited storage and transportation capacities, unreliable CCE, stochastic transportation times, stochastic demand). The simulation model is generic and can thus provide the backbone of a decision support tool that can be used to investigate various settings and interventions on the ground.

We find that substantial inequalities in full vaccination coverage exist between rainy and non-rainy season affected facilities, and between facilities in general in the current Malagasy VSC. These public health outcomes are induced by two main drivers: (i) rainy season disruptions, and (ii) operational inefficiencies (i.e., transportation capacity bottleneck). We therefore investigate two shorter-term modifications to the system: (i) introducing a rainy season buffer for the rainy season affected facilities, and (ii) increasing the replenishment frequency. Our results show that implementing a 100% rainy season buffer and introducing monthly shipments results in a 38% increase in the number of children that can be reached with all basic vaccinations. Moreover, inequalities between rainy and non-rainy season affected facilities are substantially reduced.

Our results also highlight the significant and important potential impact of an increase in flooding due to climate change on the public health performance of the current Malagasy VSC. In the absence of policy action to make the VSC more robust, even a moderate increase in flooding will result in a significant 37% increase in the number of rainy season affected facilities and, in turn, is estimated to decrease the national full vaccination coverage, resulting in a 4% reduction in fully vaccinated children. Moreover, the burden of this reduction falls disproportionally on the rainy season affected facilities with a widening of the inequality gap between rainy and non-rainy season affected facilities. Although implementing a 100% rainy season buffer and monthly shipments is still effective, it cannot prevent some deterioration in full vaccination coverage and inequalities.

Our findings have implications for policy and practice. Given the limited resources in these settings, it seems important to first focus on shorter-term modifications as such interventions are estimated to already substantially improve the public health performance of the current Malagasy VSC, and can be realized with minimal efforts and resources. However, with respect to mitigating the impact of an increase in flooding due to climate change, these shorter-term interventions will not suffice, and it seems necessary to investigate additional longer-term actions in the future. Moreover, we emphasize the importance of considering equity measures in the analysis, as a trade-off might exist between full vaccination coverage (or other health

performance indicators) and equity measures.

6.2 Limitations

Although our aim is to model reality as closely as possible, full information is mostly not available and some assumptions need to be taken. We therefore provide a brief discussion of the most important assumptions and limitations of our study.

First, as explained in Section 4.2.1, it is possible that boxes need to be discarded due to cold chain failures or insufficient storage capacity, that the number of ordered boxes can only partially be fulfilled due to insufficient vehicle capacity at the higher level facility, or that the number of ordered boxes need to be reduced due to insufficient storage space at the lower level facility. To the best of our knowledge, no detailed information is available on how these numbers are determined for each of the vaccine antigens in practice. We therefore assume that these are proportional to the volumes that were stored or ordered. This assumption is based on an equitable distribution of vaccine antigens (based on guidelines of the WHO that focus on equitable solutions, and on SDG 3.8 that aims to provide equitable access to vaccines for all). Moreover, we believe that on average, this is a reasonable assumption, as a preference for one vaccine antigen in a particular facility will likely be compensated by a focus on other vaccine antigens in other facilities.

Second, some required input data could not be extracted from the field data provided by UNICEF Madagascar, WHO information, or spatial models, and are therefore based on relevant literature, expert opinions, observations during field studies in SSA, and our own rationale. These include the failure and repair times of CCE, the random cancellations of national supply, the coefficients of variation and the ratio between the minimum and the average of the transportation times, and the number of vaccination days per week. An overview of the data sources and rationale applied to estimate these input parameters are provided in Appendix B.

Third, in our model, we include all eligible children in the demand, and we assume that people go the the nearest health facility (i.e., they minimize their travel time). Although reaching all eligible children is the ultimate goal of international organizations such as the WHO and GAVI (e.g., Reach Every District/Reach Every Child) and it is the aim of SDG 3.8 (i.e., provide access to vaccines for all), this is currently not the case in reality. Also, people might not go to the health facility that is closest to where they live, but e.g. go to the one that is on their way to work. However, no accurate data on demand for vaccinations is

available, and forecasting this demand is very difficult because of numerous influencing factors (e.g., operational, behavioral, social). Given that the aim of SDG 3.8 is to provide access to vaccines for all children, we therefore focus on the performance of the Malagasy VSC in case of maximum demand (i.e., based on the population). This means that the rationale behind the modeled demand is that there should be a vaccine available for every child. In this way, we can understand from the supply side what it takes to get full immunization. Note, however, that any demand, once available, can be easily linked to our simulation model.

Last, even though we focus on shorter-term mitigation strategies that can be realized with minimal efforts and resources, it is important to remark that these strategies still come at a cost. That is, while implementing inventory buffers and increasing replenishment frequencies result in more vaccines flowing through the supply chain, it will unavoidably increase variable holding and transportation costs. This trade-off is not that surprising. However, the magnitude of the improvement in full vaccination coverage and inequalities is remarkable.

6.3 Future work

Our paper opens several future research opportunities that are related to this work.

Extending the modeling approach to other problems and settings. Since the simulation model is generic, it can be easily adapted and applied to other problems and settings. Also, GIS and spatial modeling can be used to estimate several types of geographically related data. Future research might extend this work to other countries, or use it to investigate other types of interventions (e.g., longer-term actions to mitigate the impact of climate change). The modeling approach applied in this paper might also be extended to other types of global/public health supply chains (e.g., medicines, food), and to other types of geographical problems (e.g., droughts, snow) or disasters (e.g., hurricanes, landslides).

Embedding the modeling approach into an optimization framework. Our modeling approach might also be extended by embedding it in an optimization framework. For instance, the replenishment frequencies and rainy season buffers might be varied between different facilities to optimally use the available resources. It would also be interesting to study the optimal allocation of a limited budget to several types of supply chain investments to maximize climate change resiliency.

Understanding and modeling the demand for vaccinations. Demand for vaccinations is challenging to model because it depends on numerous influencing factors including operational,

behavioral and social factors. Comprehensive data collection and empirical analysis can help to understand and forecast the demand for vaccinations. To do so, modeling the link with other SDGs (e.g., poverty, nutrition, education) is important as these can greatly influence the demand for health care, and vaccinations specifically. These forecasts could be linked to our models to investigate a more detailed impact on public health performance.

Acknowledgements

The authors thank UNICEF Madagascar, and in particular Andry Fidele Ravalitera, for providing data, information and clarifications regarding the problem setting. The authors are also grateful for the exploratory work done by two master students, Dana Van Hout (Van Hout, 2019) and Sarah Dewilde (Dewilde, 2018).

Funding

K. De Boeck is funded by a PhD fellowship from the Research Foundation – Flanders. This work was also supported by the GlaxoSmithKline Research Chair on Re-Design of Healthcare Supply Chains in Developing Countries to increase Access to Medicines.

Appendix

A Details modeling approach

The discrete-event simulation model was programmed in AnyLogic 8.4.0. The spatial models were developed using QGIS 3.4.12.

A.1 Discrete-event simulation model

This subsection provides a detailed overview of the discrete-event simulation model structure. An overview of the notations used throughout this subsection is given in Table 7.

A box b that contains a specified number of vaccine vials v is transported between and stored at facilities throughout the VSC. These facilities can be either storage facilities j at the national, regional and district levels, or basic health centers h at the lowest level of the supply chain. Administration of vaccines only occurs at the basic health centers h. Transportation between storage facilities j is conducted using one of the available transportation modes l. Each vaccine antigen i differs with respect to the number of doses per vial d_i, the number of doses required to be fully vaccinated a_i, the packed volume per vial q_i, the wastage rate w_i as defined by the WHO and, for multi-dose vials, whether there is open-vial wastage (i.e., whether the multi-dose vial cannot be used anymore after opening) o_i.

The model is instantiated for 8 vaccine antigens i, 129 storage facilities j, 3155 basic health centers h, and 4 transportation modes l, where

$$\begin{aligned} &i \in \{\text{BCG, DTC-HepB-Hib, IPV, OPV, MMR, PCV-10, ROTA, TT}\}, \\ &l \in \{\text{airplane, truck, pickup, motorcycle}\}. \end{aligned} \tag{2}$$

The model logic consists of four main parts: (i) the supply of vaccines at the national level, (ii) the reception and storage of vaccines at the storage facilities j, (iii) the reception, handling and execution of orders at facilities j, and (iv) the ordering process and the demand at the basic health centers h. The remainder of this subsection defines the dynamics of each of these four parts.

Table 7: Model notation summary

I/O	Notation	Definition
Inputs	i	Vaccine antigen
	j	Storage facility
	h	Basic health center
	l	Transportation mode
	r	Transportation route
	y	Vaccination day
	v	Number of vaccine vials per box
	d_i	Number of doses per vial for vaccine antigen i
	a_i	Number of doses required to be fully vaccinated for vaccine antigen i
	q_i	Packed volume per vial for vaccine antigen i
	w_i	Wastage rate for vaccine antigen i as defined by the WHO
	o_i	Binary parameter indicating, for multi-dose vials, whether there is open-vial wastage for vaccine antigen i
	λ_n	National replenishment rate
	λ_c	Maximum cancellation rate national replenishment
	N_j^c	Number of cold rooms at facility j
	N_j^f	Number of fridges at facility j
	C^c	Net storage capacity (in liters) of a cold room
	C^f	Net storage capacity (in liters) of a fridge
	C_j^{init}	Initial storage capacity (in liters) at facility j
	t_f	Mean failure time of fridges
	t_r	Mean repair time of fridges
	t_r^{max}	Maximum repair time of fridges
	t_r^{min}	Minimum repair time of fridges
	λ_r	Rate at which facilities are replenished
	M_{ji}	Order-up-to level (in boxes) of facility j for vaccine antigen i
	N_{jl}^t	Number of transportation mode l available at facility j
	C_l^t	Net storage capacity (in liters) of transportation mode l
	t_{kjl}	Mean transportation time from facility k to facility j using transportation mode l
	t_{kjl}^{min}	Minimum transportation time from facility k to facility j using transportation mode l
	CV_l	Coefficient of variation of transportation mode l
	w_l^t	Percentage of boxes that is lost during transportation using transportation mode l
	τ	Factor by which t_kjl^{min} increases during the rainy season
	λ_{ih}^d	Mean demand rate for vaccine antigen i at basic health center h
	D_{ih}^{max}	Maximum yearly demand (in doses) for vaccine antigen i at basic health center h
	λ_p	Rate at which basic health centers pick up boxes at the supplying storage facility
	M_{hi}	Order-up-to level (in boxes) of basic health center h for vaccine antigen i
	$\mathbb{E}[D_{hi}]$	Average forecasted demand during the replenishment period for vaccine antigen i at basic health center h
	s	Safety factor s for order-up-to-levels as determined by the WHO
Intermediary outputs	I_{ji}	Inventory level (in boxes) of vaccine antigen i at facility j
	C_j^{eff}	Effective storage capacity (in liters) at facility j
	C_j^{req}	Required storage capacity (in liters) at facility j
	B_{ji}^f	Number of discarded boxes of vaccine antigen i when a CCE failure occurs at storage facility j
	b_{ji}^f	Number of boxes of vaccine antigen i that was stored at facility j before the CCE failure
	B_{ji}^r	Number of discarded boxes of vaccine antigen i from a replenishment at facility j
	b_{ji}^r	Number of boxes of vaccine antigen i that is present in the replenishment at facility j
	O_{kji}	Ordered boxes of vaccine antigen i ordered by lower-level facility j at higher-level facility k
	B_{kji}^o	Number of boxes by which the ordered quantities O_{kji} for each vaccine antigen i are reduced in case of insufficient storage capacity at facility j
	b_{kji}^o	Number of boxes of vaccine antigen i that were planned to be ordered by facility j at facility k
	S_{kji}	Shipped boxes of vaccine antigen i from facility k to facility j
	C_r^o	Total required capacity (in liters) of all orders included in route r
	S_{kir}^{total}	Total shipped boxes from facility k of each vaccine antigen i on route r
	B_{kir}^s	Number of boxes by which the total shipped quantities S_{kir}^{total} for each vaccine antigen i are reduced in case of insufficient transportation capacity
	b_{kir}^s	Number of boxes of vaccine antigen i that were planned to be shipped from facility k on transportation route r
	D_{ih}^{total}	Total yearly demand (in doses) for vaccine antigen i at basic health center h
	d_{hiy}^d	Demand (in doses) for vaccine antigen i at basic health center h on vaccination day y
	I_{hi}	Inventory level (in boxes) of vaccine antigen i at basic health center h
	I_{hi}^v	Inventory level (in vials) of vaccine antigen i at basic health center h
	d_{hiy}^v	Number of demanded vials of vaccine antigen i on vaccination day y at basic health center h
	u_{hiy}^v	Number of used vials of vaccine antigen i on vaccination day y at basic health center h
	O_{hi}	Ordered boxes of vaccine antigen i by basic health center h
	P_{hi}	Number of boxes that are eventually picked up by the basic health center h for each vaccine antigen i

A.1.1 National supply

The national storage facility is replenished at a specified rate λ_n (i.e., trimestral in our case study). The first replenishment in the simulation model occurs at time $t = \text{uniform}(0, \frac{1}{\lambda_n})$. Because of delays in the procurement process, it is possible that a replenishment is not fulfilled (i.e., the replenishment is canceled). This happens at a rate that follows a uniform distribution with maximum λ_c, thus occurring at most one time per $\frac{1}{\lambda_c}$ years.

A.1.2 Reception and storage of vaccines at the storage facilities j

Each storage facility j has a number of cold rooms N_j^c and fridges N_j^f with a net capacity of C^c and C^f liters, respectively. However, a significant proportion α_j of the fridges at facility j can be obsolete. This means that each facility j has an initial storage capacity C_j^{init} equal to

$$C_j^{init} = N_j^c C^c + (1 - \alpha_j)(N_j^f C^f). \tag{3}$$

Fridges fail after a life period that follows an exponential distribution with a mean t_f. The time to repair follows a triangular distribution with a mean t_r, a maximum t_r^{max} and a minimum t_r^{min}. Due to these cold chain failures, the effective capacity C_j^{eff} might be substantially lower than the initial capacity C_j^{init}. Moreover, when a CCE failure occurs, the resulting effective capacity C_j^{eff} might be smaller than the required capacity C_j^{req} to store all boxes of vaccines currently present at facility j, and some boxes are therefore discarded. The number of discarded boxes B_{ji}^f for the different vaccine antigens i when a CCE failure occurs at storage facility j is proportional to the number of boxes b_{ji}^f that was stored at facility j before the CCE failure occurred and the packed volume per vial q_i, where

$$B_{ji}^f = \left\lceil \frac{b_{ji}^f v q_i}{\sum_{i \in I} b_{ji}^f v q_i} (C_j^{req} - C_j^{eff}) \frac{1}{q_i} \frac{1}{v} \right\rceil. \tag{4}$$

The resulting inventory I_{ji} of vaccine antigen i at facility j after a CCE failure thus equals

$$I_{ji} = I_{ji} - B_{ji}^f. \tag{5}$$

To account for local practices at many storage facilities in response to cold chain problems with respect to insufficient storage space (e.g., transporting vaccines to the nearest facility and retrieving the vaccines right before vaccination sessions), we assume that there is always at least

one fridge working at each facility j.

Upon reception of a replenishment of vaccines at storage facility j, it is checked whether there is enough storage space available to store all the arrived boxes. When this is not the case (i.e., the effective capacity C_j^{eff} is smaller than the required capacity C_j^{req} to store all boxes of vaccines currently present at facility j), some of the replenished boxes are discarded. The number of discarded boxes B_{ji}^r for the different vaccine antigens i is proportional to the number of boxes b_{ji}^r that is present in the replenishment and the packed volume per vial q_i, where

$$B_{ji}^r = \left\lceil \frac{b_{ji}^r v q_i}{\sum_{i \in I} b_{ji}^r v q_i} (C_j^{req} - C_j^{eff}) \frac{1}{q_i} \frac{1}{v} \right\rceil . \tag{6}$$

The resulting inventory I_{ji} of vaccine antigen i at facility j after a replenishment of b_{ji}^r boxes thus equals

$$I_{ji} = \begin{cases} I_{ji} + b_{ji}^r & \text{if } C_j^{eff} \geq C_j^{req}, \\ I_{ji} + \left(b_{ji}^r - B_{ji}^r \right) & \text{if } C_j^{eff} < C_j^{req}. \end{cases} \tag{7}$$

A.1.3 Reception, handling and execution of orders at the storage facilities j

Each storage facility j at the regional and district level is replenished at a rate λ_r and has an order-up-to level M_{ji} for each vaccine antigen i. The ordered quantities O_{kji} of vaccine antigen i ordered by lower-level facility j at higher-level facility k equal

$$O_{kji} = M_{ji} - I_{ji}. \tag{8}$$

However, it is possible (e.g., due to fridge breakdowns) that there is not enough storage space left at facility j to store all the planned ordered vaccines (i.e., the effective capacity C_j^{eff} is smaller than the required capacity C_j^{req} to store the sum of all boxes of vaccines currently present at facility j and the planned ordered vaccines). In this case, the ordered quantities O_{kji} for each vaccine antigen i are reduced with B_{kji}^o, proportionally to the number of boxes b_{kji}^o that was planned to be ordered and the packed volume per vial q_i, where

$$B_{kji}^o = \left\lceil \frac{b_{kji}^o v q_i}{\sum_{i \in I} b_{kji}^o v q_i} (C_j^{req} - C_j^{eff}) \frac{1}{q_i} \frac{1}{v} \right\rceil . \tag{9}$$

The resulting ordered quantities then equal

$$O_{kji} = O_{kji} - B^{o}_{kji}. \tag{10}$$

The handling of orders at the supplying facilities only happens during working hours. For a single-destination route, the shipped quantities S_{kji} of vaccine antigen i from upper level facility k to lower level facility j are determined based on the inventory levels I_{ki} where

$$S_{kji} = min\left\{O_{kji}, I_{ki}\right\}. \tag{11}$$

When multiple facilities are included in a transportation route r, and the inventory at the supplying facility is enough to cover all orders, the shipped quantities S_{kji} are determined in the same way as for the single-destination routes. However, when the sum of the ordered quantities O_{kji} exceeds the current stock of the supplying facility, the shipped quantities S_{kji} are determined proportionally to the ordered quantities O_{kji} where

$$S_{kji} = \left\lfloor \frac{O_{kji}}{\sum_{j \in r} O_{kji}} I_{ki} \right\rfloor. \tag{12}$$

Each facility j has a number N^{t}_{jl} of transportation mode l available, each with a net capacity of C^{t}_{l}. The transportation mode l that is used to deliver the order depends both on the availability of the transportation modes and the total required capacity C^{o}_{r} of all orders included in the route where

$$C^{o}_{r} = \sum_{j \in r} \sum_{i \in I} O_{kji} q_i v. \tag{13}$$

To determine the transportation mode l that is used to execute the deliveries, it is first checked whether a transportation mode l is available that has a net capacity C^{t}_{l} greater or equal to the total required capacity C^{o}_{r}. Next, if no such transportation mode is currently available, the transportation mode with the greatest net capacity that is currently idle at facility k is selected. Last, if no transportation modes are currently idle at facility k, the orders are canceled.

In case the net capacity C^{t}_{l} of the selected transportation mode l is smaller than the total required capacity C^{o}_{r}, the total shipped quantities S^{total}_{kir} on route r for each vaccine antigen i are

reduced with B^s_{kir}, proportionally to the number of boxes b^s_{kir} that was planned to be shipped and the packed volume per vial q_i, where

$$B^s_{kir} = \left\lceil \frac{b^s_{kir} v q_i}{\sum_{i \in I} b^s_{kir} v q_i} (C^o_r - C^t_l) \frac{1}{q_i} \frac{1}{v} \right\rceil, \tag{14}$$

$$S^{total}_{kir} = S^{total}_{kir} - B^s_{kir}, \tag{15}$$

$$S_{kji} = \left\lfloor \frac{O_{kji}}{\sum_{j \in r} O_{kji}} S^{total}_{kir} \right\rfloor. \tag{16}$$

After the shipped quantities S_{kji} are determined, the route is executed. We assume that transportation times follow a lognormal distribution with a minimum t^{min}_{kjl}, a mean t_{kjl} and a coefficient of variation CV_l, depending on the transportation mode l. Drivers only depart from a facility to continue their route during working hours. Also, during transportation, a percentage w^t_l of the vaccines is lost due to e.g. breakage, depending on the transportation mode l.

The presence of the rainy season complicates the delivery of vaccines. Some facilities are not accessible, and are therefore not replenished during the rainy season. Moreover, we assume that the accessible facilities are also impacted by the rainy season, as the minimum transportation times t^{min}_{kjl} increase with a factor τ during this period of the year.

A.1.4 Ordering process and demand at the basic health centers h

Administration of vaccines at the basic health centers h occurs on a specified number of vaccination days per week y. The demand at each basic health center h for each vaccine antigen i on a vaccination day follows a Poisson distribution (as commonly used in literature) with a mean λ^d_{ih}. Moreover, the total yearly demand D^{total}_{ih} is capped by a maximum D^{max}_{ih} that is based on the basic health center's catchment area. We assume that demand that is not fulfilled, is lost.

In each basic health center h, on every vaccination day y, a demand d^d_{hiy} in doses is generated for each vaccine antigen i. For the basic health centers, the inventory is recorded in the simulation model both in number of boxes I_{hi} and in number of vials I^v_{hi}. Based on the demand d^d_{hiy} and the inventory levels I^v_{hi}, the number of demanded vials d^v_{hiy} and the number of used vials u^v_{hiy} on vaccination day y at basic health center h for vaccine antigen i are calculated,

where

$$d^v_{hiy} = \begin{cases} \left\lceil \frac{d^d_{hiy}}{d_i} \right\rceil & \text{if } o_i = 1, \\ \frac{d^d_{hiy}}{d_i} & \text{if } o_i = 0, \end{cases} \tag{17}$$

$$u^v_{hiy} = \begin{cases} d^v_{hiy} & \text{if } I^v_{hi} \geq d^v_{hiy}, \\ I^v_{hi} & \text{if } I^v_{hi} < d^v_{hiy}. \end{cases} \tag{18}$$

The resulting inventory I^v_{hi} of vaccine antigen i at basic health center h at the end of vaccination day y then equals

$$I^v_{hi} = I^v_{hi} - u^v_{hiy}. \tag{19}$$

Each basic health center h travels to the supplying storage facility j to pick up vaccines at a rate λ_p. To determine the required quantities O_{hi} for each vaccine antigen i, an order-up-to policy is applied. The order-up-to level M_{hi} is based on the average forecasted demand $\mathbb{E}[D_{hi}]$ during the period $\frac{1}{\lambda_p}$, and is increased by a wastage factor w_i and a safety factor s as determined by the WHO, where

$$M_{hi} = \mathbb{E}[D_{hi}] w_i s. \tag{20}$$

The quantities P_{hi} that are eventually picked up by the basic health center h for each vaccine antigen i are determined by the order-up-to levels M_{hi}, the inventory levels I^v_{hi} and I_{hi} of the basic health center h, the ordered quantities O_{hi}, and the inventory levels I_{ji} of the supplying facility j, where

$$I_{hi} = \left\lfloor \frac{I^v_{hi}}{v} \right\rfloor, \tag{21}$$

$$O_{hi} = M_{hi} - I_{hi}, \tag{22}$$

$$P_{hi} = min\left\{O_{hi}, I_{ji}\right\}. \tag{23}$$

The resulting inventory I^v_{hi} of vaccine antigen i at basic health center h then equals

$$I^v_{hi} = I^v_{hi} + P_{hi} v. \tag{24}$$

Table 8: Overview of hazard classifications for flow accumulation, slope, land use, rainfall intensity, and elevation, based on Kourgialas and Karatzas (2011) and Ozkan and Tarhan (2016)

Factor	Classification	Hazard classification
Flow accumulation (pixels)	≥ 5868	Very high (10)
	3244 – 5868	High (8)
	1908 – 3244	Moderate (5)
	620 – 1908	Low (2)
	0 – 620	Very low (1)
Slope (degrees)	0 – 3.6	Very high (10)
	3.6 – 9.6	High (8)
	9.6 – 16.2	Moderate (5)
	16.2 – 24.6	Low (2)
	≥ 24.6	Very low (1)
Land cover	Water, permanent wetland	Very high (10)
	Shrublands, urban, barren or sparsely vegetated, savannas	High (8)
	Grasslands, croplands	Moderate (5)
	Natural vegetation mosaic	Low (2)
	Forest, snow and ice	Very low (1)
Rainfall intensity (MFI)	≥ 282	Very high (10)
	237 – 282	High (8)
	197 – 237	Moderate (5)
	159 – 197	Low (2)
	0 – 159	Very low (1)
Elevation (m)	< 153	Very high (10)
	153 – 414	High (8)
	414 – 697	Moderate (5)
	697 – 1049	Low (2)
	≥ 1049	Very low (1)

A.2 Spatial models

A.2.1 Flood map

Similar to prior literature, we consider five factors that contribute to the flood hazard value: flow accumulation, slope, land use, rainfall intensity, and elevation (Ajin et al., 2013; Kourgialas and Karatzas, 2011; Ozkan and Tarhan, 2016). For each of these factors, we construct a GIS map classifying each pixel of the map of Madagascar into one of the five categories of flood hazard. An overview of the applied classifications is given in Table 8.

In order to create the final flood hazard map, a linear combination of the five GIS factor maps is calculated. The factor weights are determined by applying the method of Shaban et al. (2001) which considers the interaction between different factors. An overview of the major and minor interactions between the considered factors (i.e., flow accumulation, slope, land use,

Figure 6: Overview of the major and minor interactions between factors that form and influence a flood

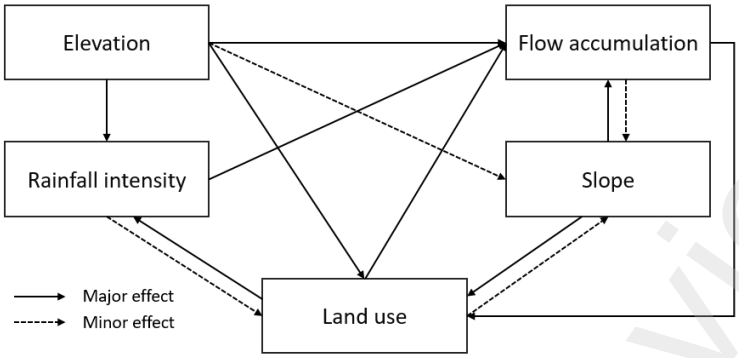

Table 9: Overview of the applied weights for the different factors

Factor	Weight (%)
Flow accumulation (pixels)	13.64
Slope (degrees)	18.18
Land cover	22.73
Rainfall intensity (MFI)	13.64
Elevation (m)	31.82

rainfall intensity, elevation), based on Kourgialas and Karatzas (2011), and Ozkan and Tarhan (2016), is given in Figure 6. A factor weight is increased with 0.5 and with 1 if it has a minor (i.e., indirect) and major (i.e., direct) effect, respectively, on another factor (e.g., if a factor has a major effect on two other factors, it is increased with 2). These weights are then converted so that they sum up to 1 in order to obtain the final weights. An overview of the applied weights can be found in Table 9.

We use open-source data to create the five GIS factor maps. The flow accumulation data are extracted from the Hydrologic Derivatives for Modeling and Applications (HDMA) database which is distributed by the US Geological Survey (USGS) (Verdin, 2017). The slope data are obtained from the KTH Royal Institute of Technology in Stockholm (KTH-dESA, 2019). This data set has a resolution of one kilometer and is calculated based on data from the Shuttle Radar Topography Mission (SRTM). The data on land use are accessed through the USGS Land Cover Institute who provide global land cover data based on Moderate Resolution Imaging Spectroradiometer data (Broxton et al., 2014). The data on rainfall intensity are calculated from precipitation data provided by Worldclim (Fick and Hijmans, 2017). These precipitation data

have a resolution of one kilometer and include the average monthly rainfall. To obtain the rainfall intensity, we calculate the modified fournier index (MFI) (Morgan, 2005):

$$MFI = \sum_{t=1}^{12} \frac{p_t^2}{P}, \tag{25}$$

where p_t is the average monthly rainfall in month t and P is the average annual rainfall. The elevation data are released by the geospatial science community of the Consultative Group of International Agricultural Research (CGIAR-CSI, 2019). Similar to the slope data set, it is based on data from the SRTM and it has a resolution of 90 meter.

Applying the method outlined above, we obtain the five individual factor maps (Figure 7) and the consolidated flood hazard map (Figure 2 in Section 4.3.1).

A.2.2 Rainy season disruptions

Figure 8 gives an overview of the rainy season affected storage facilities when the method explained in Section 4.3.3 is applied.

A.2.3 Geographical allocation of demand to basic health centers

Figure 9 shows the catchment areas of the basic health centers and the corresponding travel times (during the dry season) to the nearest health center. These are obtained by applying the method outlined in Section 4.3.4.

B Overview input data

Table 10 provides an overview of the data sources used to estimate the input parameters. The different data sources used are: (i) field data including raw data, reports, and discussions with collaborators, (ii) WHO information as available on the WHO website, (iii) spatial models as explained in Section 4.3, (iv) relevant literature, (v) expert opinions, (vi) observations and interviews during field studies in SSA, and (vii) own rationale. As can be seen in Table 10, 74% of the input parameters are entirely based on field data, WHO information and spatial models (i.e., based on private or publicly available data), and only 8% is determined based on our own rationale.

For each of the input parameters based on relevant literature, expert opinions, observations during field studies, or our own rationale, we provide a short explanation.

Figure 7: Factor maps of (a) flow accumulation, (b) slope, (c) land cover, (d) rainfall intensity, and (e) elevation

(a) Flow accumulation

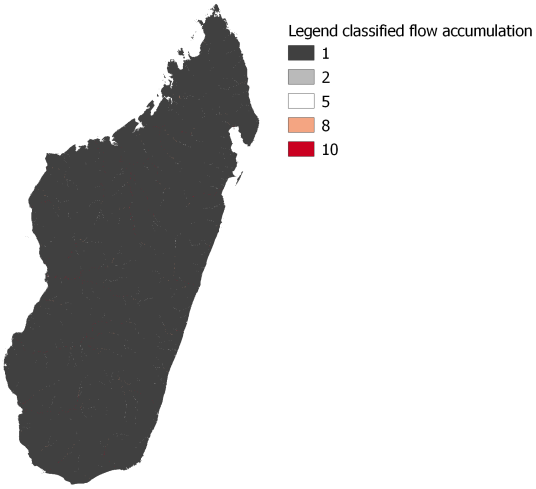

(b) Slope

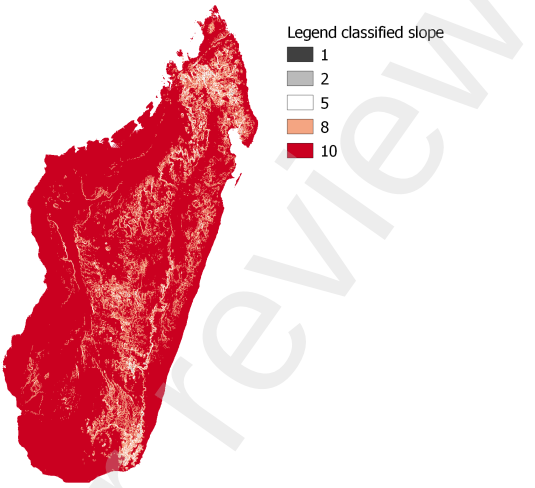

(c) Land cover

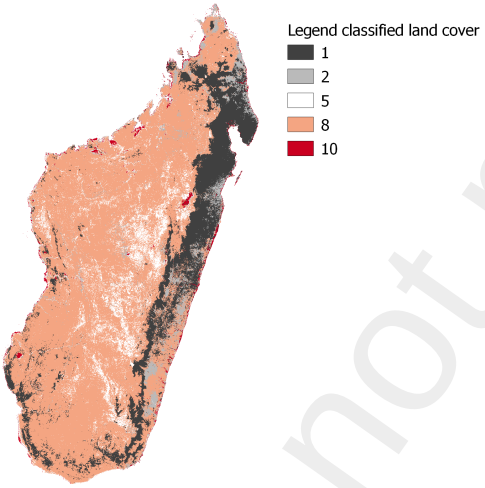

(d) Rainfall intensity

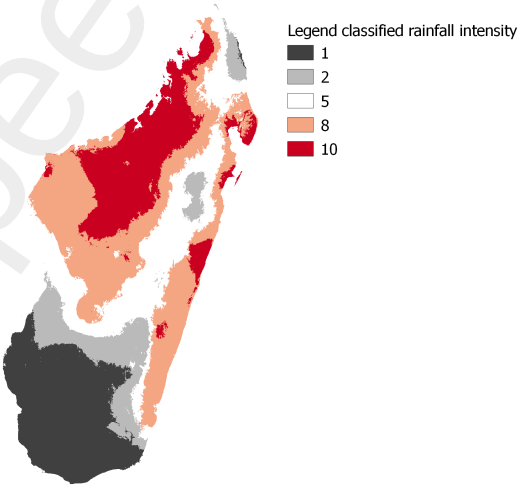

(e) Elevation

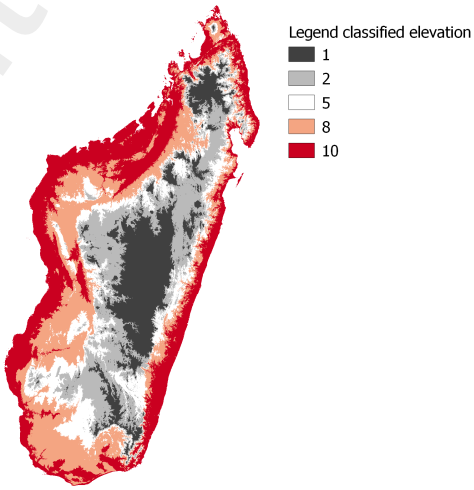

Figure 8: Overview of the rainy season affected storage facilities

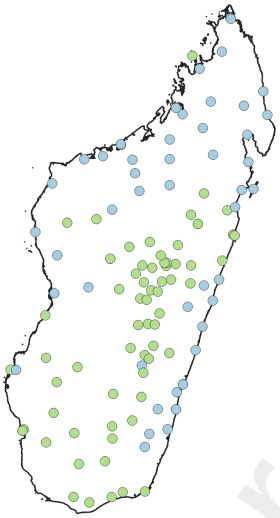

Notes: Facilities that are affected by the rainy season are indicated in blue.

Figure 9: (a) Catchment areas of basic health centers and (b) corresponding travel times to the nearest basic health center

(a) Catchment areas of basic health centers (b) Travel times to nearest basic health center

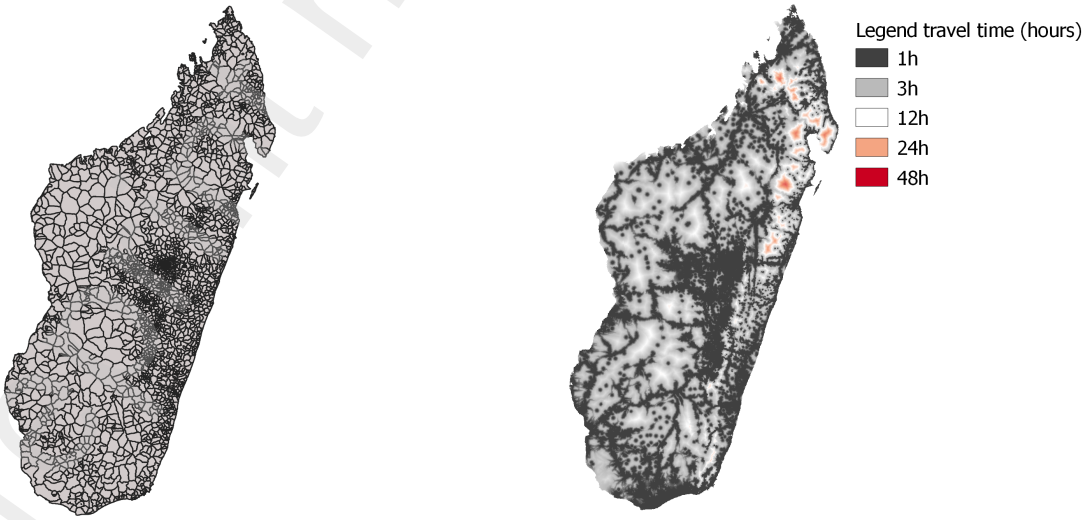

Table 10: Overview of data sources used to estimate input parameters

Input parameter	Data source used
i	field data
j	field data
h	field data, spatial models
l	field data
r	field data
y	observations during field studies
v	WHO information
d_i	WHO information
a_i	WHO information
q_i	WHO information
w_i	WHO information
o_i	WHO information
λ_n	field data
λ_c	observations during field studies
N_j^c	field data
N_j^f	field data
C^c	field data, WHO information
C^f	field data, WHO information
C_j^{init}	field data, WHO information
t_f	expert opinion, observations during field studies
t_r	expert opinion, observations during field studies
t_r^{max}	expert opinion, observations during field studies
t_r^{min}	expert opinion, observations during field studies
λ_r	field data
M_{ji}	field data, spatial models
N_{jl}^t	field data
C_l^t	field data, WHO information
t_{kjl}	spatial models, own rationale
t_{kjl}^{min}	spatial models
CV_l	own rationale
w_l^t	relevant literature
τ	own rationale
λ_{ih}^d	spatial models
D_{ih}^{max}	spatial models
λ_p	field data
M_{hi}	field data, WHO information, spatial models
$\mathbb{E}[D_{hi}]$	spatial models
s	WHO information

Notes: The definitions of the different input parameters are given in Table 7 in Appendix A.1.

Number of vaccination days y. The number of vaccination days per week might vary between different health facilities, as it is based on several factors including the number of children in the catchment area, the distances to the health center (determining outreach actions), and the availability of health care staff. During field studies in SSA, we observed that most health facilities try to concentrate the vaccinations per vaccine antigen on a fixed weekday to minimize open-vial wastage. Also, most health facilities perform outreach sessions once a week. Therefore, y equals 2 days per week in the simulation model.

Maximum national replenishment cancellation rate λ_c. Cancellations of national vaccine deliveries are reported during interviews and field studies. However, their frequency is often unknown and/or volatile. Based on interviews and field studies and due to limited information, we use a uniform distribution with a maximum cancellation rate of 0.25. This means that it occurs at most one time per 4 years. An interesting future research area might be to model the occurrence and drivers of cancellations of national vaccine deliveries. This model might then be connected to our simulation model to investigate the impact of these cancellations on public health performance (e.g., a studie similar to Gallien et al. (2017) who build a simulation model to predict the joint impact of procurement and grant disbursement processes on national drug availability in Africa).

Failure and repair times of fridges. The average life expectancy (and thus failure time) of a fridge is 5 years. However, due to the conditions these fridges are used in, the time until failure might also be considerably shorter. We therefore use an exponential distribution with a mean t_f of 5 years to simulate fridge failures. When a fridge breaks down, it can either be repaired or replaced. Reparations can take a long time as there is often only a limited number of technicians responsible for a region (or country). Moreover, when a fridge needs to be replaced, this can take years. We therefore model the time to repair by a triangular distribution with a mean t_r of 12 months, a minimum t_r^{min} of 3 months and a maximum t_r^{max} of 36 months. The lack of data on failure and repair times of CCE in LMICs, and the drivers behind it provide an interesting research area for future empirical research.

Data regarding the statistical distribution of transportation times. No field data is currently available regarding the road network or transportation times between facilities in Madagascar. By defining the road network through spatial modeling (Section 4.3.2), we obtain good estimates of the best-case (i.e., minimum) transportation times. Based on literature (Hao et al., 2013; Mazloumi et al., 2010; Srinivasan et al., 2014), we use a lognormal distribution to simulate the

transportation times. In order to do so, we use the minimum transportation time t_{kjl}^{min}, the average transportation time t_{kjl}, and the coefficients of variation CV_l. We then characterize the parameters μ and σ^2 of the lognormal distribution (with μ and σ^2 being the mean and variance of the included normal distribution) of the transportation times as follows (Vandaele, 1996):

$$\mu_{kjl} = \ln\left(\frac{t_{kjl}}{\sqrt{CV_l^2 + 1}}\right), \tag{26}$$

$$\sigma_{kjl}^2 = \ln\left(CV_l^2 + 1\right). \tag{27}$$

We then apply the following probability density function:

$$f\left(t_{kjl}\right) = \frac{1}{\left(t_{kjl} - t_{kjl}^{min}\right)\sqrt{2\pi\sigma_{kjl}^2}} \exp\left(-\frac{\left(\ln\left(t_{kjl} - t_{kjl}^{min}\right) - \mu_{kjl}\right)^2}{2\sigma_{kjl}^2}\right). \tag{28}$$

In the simulation model, the squared coefficients of variation CV_l^2 equal 0.5, and the minimum transportation times t_{kjl}^{min} are increased with 20% and 30% to obtain the average transportation times t_{kjl} during the dry and rainy season, respectively. Furthermore, we set τ (i.e., the factor by which t_{kjl}^{min} increases during the rainy season) equal to $\frac{5}{3}$.

Percentage of boxes lost during transportation w_l^t. Although it is indicated in literature (De Boeck et al., 2019) and during field studies that vaccine vials are lost or broken during transportation, no detailed data is currently available. We therefore define these percentages based on relevant literature (Assi, 2011): 1% and 2% of boxes is lost during transportation by airplane or (cold) truck, and during transportation by pickup or motorcycle, respectively.

C Validation spatial maps

First, Figure 10 shows the categorized flood hazard map that is made available by OasisHub (OasisHub, 2019; Climate-ADAPT, 2019) and the flood map that we constructed in Section 4.3.1. The areas and degrees of risk indicated by the two maps are similar (by visual inspection).

Second, Figure 11 depicts the road infrastructure provided by the LCA (LCA, 2019a,b) and the road network during the dry season that we developed in Section 4.3.2. As is clear from Figure 11, the two road networks are almost identical.

Figure 10: Categorized flood hazard map (a) made available by OasisHub (OasisHub, 2019), and (b) that we constructed in Section 4.3.1

(a) Flood map OasisHub

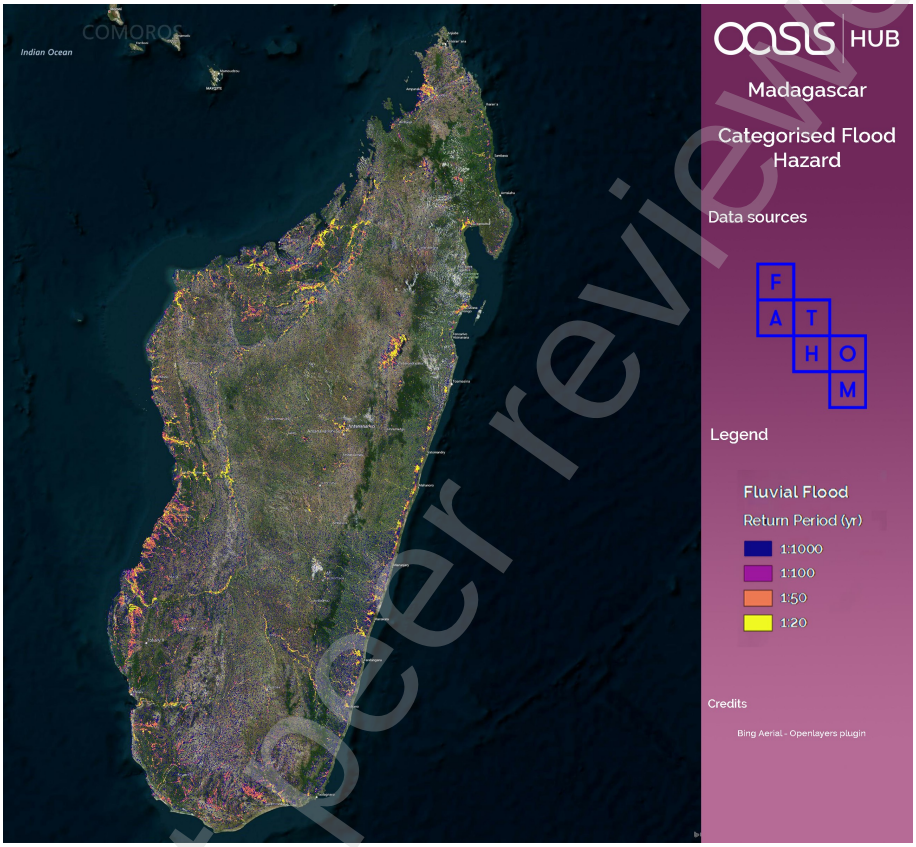

(b) Flood map constructed in Section 4.3.1

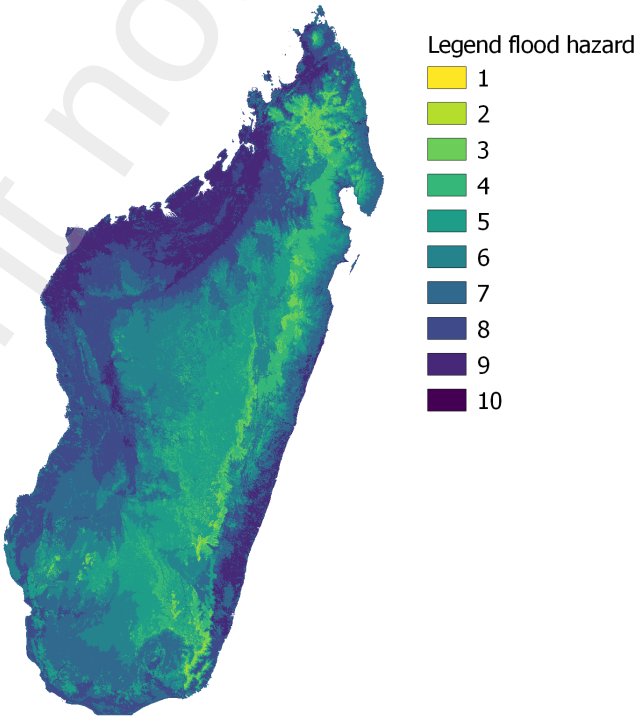

Figure 11: Overview of (a) the Malagasy road network, obtained from the LCA tool (LCA, 2019b), and (b) the road network during the dry season that we developed in Section 4.3.2.

(a) Road network LCA tool

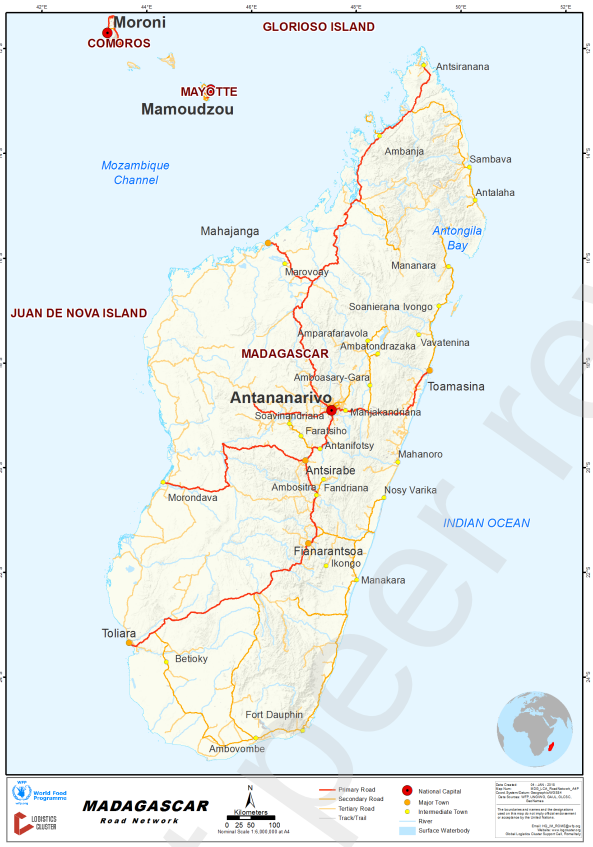

(b) Road network constructed in Section 4.3.2

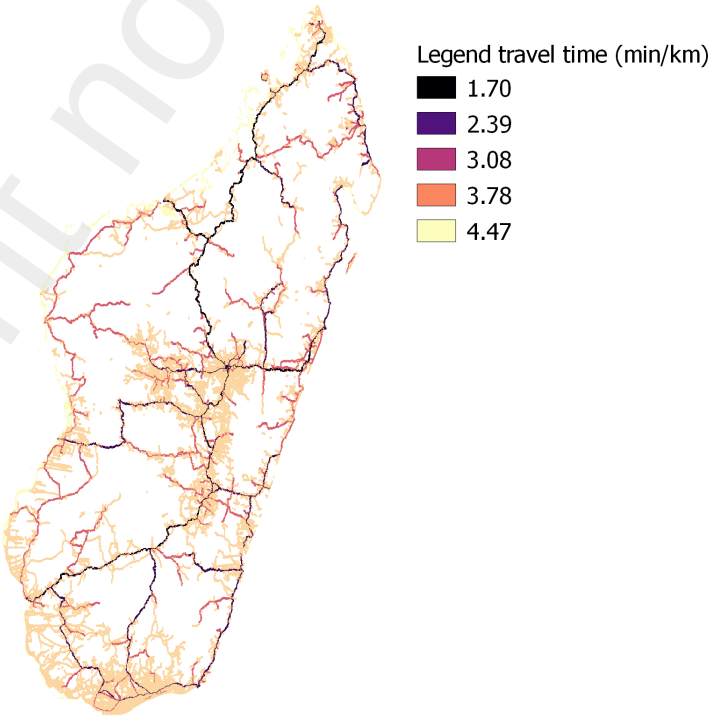

D Additional model results

The simulated model outputs, including the simulated averages and 95% confidence intervals for each of the simulated scenarios in this paper are given in Table 11.

Table 11: Additional simulation outputs of the current Malagasy VSC, the impact of climate change and the modifications

Shipping frequency		1 month						2 months						3 months					
Rainy season buffer		No buffer		50%		100%		No buffer		50%		100%		No buffer		50%		100%	
		Mean	95% CI	Mean	95% CI	Mean	95% CI	Mean	95% CI	Mean	95% CI	Mean	95% CI	Mean	95% CI	Mean	95% CI	Mean	95% CI
Current rainy season	Public health performance																		
	α_{tot} (%)	79.93	[79.43; 80.43]	83.12	[82.59; 83.65]	85.03	[84.53; 85.54]	75.24	[74.67; 75.81]	77.30	[76.85; 77.74]	78.71	[78.34; 79.07]	61.63	[61.44; 61.81]	62.15	[61.95; 62.35]	62.55	[62.34; 62.76]
	α_R (%)	57.87	[57.34; 58.39]	66.89	[66.37; 67.42]	72.29	[71.85; 72.72]	54.22	[53.51; 54.93]	59.33	[58.71; 59.94]	62.65	[62.11; 63.19]	42.96	[42.61; 43.32]	45.53	[45.10; 45.96]	46.42	[46.01; 46.84]
	α_{NR} (%)	89.93	[89.35; 90.51]	90.47	[89.84; 91.11]	90.80	[90.20; 91.40]	84.74	[84.16; 85.33]	85.41	[84.95; 85.87]	85.95	[85.55; 86.35]	70.05	[69.82; 70.27]	69.64	[69.43; 69.86]	69.82	[69.62; 70.02]
	MAD_{fac} (%)	17.23	[17.02; 17.44]	12.99	[12.78; 13.20]	10.87	[10.72; 11.01]	20.65	[20.44; 20.87]	19.31	[19.08; 19.55]	19.94	[19.72; 20.17]	24.71	[24.51; 24.90]	26.11	[25.91; 26.30]	27.07	[26.88; 27.26]
	MAD_R (%)	16.03	[15.76; 16.30]	11.79	[11.48; 12.09]	9.26	[9.01; 9.51]	15.26	[14.99; 15.53]	13.04	[12.77; 13.31]	11.65	[11.37; 11.93]	13.54	[13.32; 13.76]	12.06	[11.82; 12.29]	11.70	[11.49; 11.90]
	Operational performance																		
	W_{CCE} (boxes)	61	[44; 77]	88	[71; 105]	174	[146; 202]	301	[265; 336]	433	[383; 482]	510	[464; 557]	373	[329; 416]	429	[385; 473]	383	[344; 422]
	W_{tr} (boxes)	2295	[2278; 2312]	2412	[2392; 2431]	2490	[2473; 2508]	2127	[2108; 2146]	2209	[2190; 2228]	2243	[2228; 2259]	1682	[1671; 1693]	1694	[1683; 1705]	1703	[1693; 1713]
	MO_{inv} (boxes)	15503	[14030; 16977]	15752	[13966; 17538]	16758	[15054; 18462]	16578	[14878; 18277]	20514	[19063; 21965]	26782	[25398; 28166]	22292	[21812; 22771]	30397	[29821; 30973]	39108	[38368; 39849]
	MO_{veh} (boxes)	10559	[9885; 11234]	11324	[10596; 12053]	11799	[11160; 12438]	1445	[1134; 1757]	1487	[1113; 1861]	1062	[838; 1285]	162	[79; 245]	233	[123; 342]	254	[134; 374]
	MO_{cap} (boxes)	1680	[1587; 1773]	2540	[2406; 2674]	4021	[3848; 4195]	9154	[8824; 9485]	14491	[14069; 14914]	19277	[18801; 19753]	29745	[29320; 30171]	35893	[35382; 36404]	39451	[38912; 39989]
Climate change	Public health performance																		
	α_{tot} (%)	76.12	[75.54; 76.69]	80.86	[80.39; 81.32]	82.56	[81.93; 83.18]	71.75	[71.44; 72.07]	73.32	[72.87; 73.77]	74.62	[74.28; 74.96]	58.98	[58.76; 59.19]	59.67	[59.44; 59.91]	59.79	[59.55; 60.03]
	α_R (%)	57.66	[57.13; 58.20]	66.86	[66.43; 67.30]	71.46	[70.89; 72.03]	53.30	[52.83; 53.78]	57.88	[57.34; 58.43]	60.81	[60.29; 61.32]	41.57	[41.20; 41.95]	43.35	[42.96; 43.74]	44.02	[43.66; 44.37]
	α_{NR} (%)	89.62	[88.91; 90.33]	91.09	[90.51; 91.67]	90.67	[89.93; 91.41]	85.24	[84.91; 85.56]	84.59	[84.10; 85.08]	84.70	[84.33; 85.07]	71.68	[71.46; 71.91]	71.58	[71.33; 71.83]	71.30	[71.00; 71.59]
	MAD_{fac} (%)	18.57	[18.33; 18.81]	13.92	[13.74; 14.10]	11.91	[11.74; 12.09]	21.74	[21.54; 21.93]	20.99	[20.77; 21.21]	22.62	[22.39; 22.85]	25.04	[24.87; 25.22]	27.07	[26.87; 27.26]	28.38	[28.19; 28.57]
	MAD_R (%)	15.98	[15.69; 16.27]	12.11	[11.88; 12.34]	9.61	[9.34; 9.87]	15.97	[15.73; 16.20]	13.35	[13.10; 13.61]	11.95	[11.68; 12.21]	15.06	[14.85; 15.26]	14.11	[13.90; 14.33]	13.64	[13.42; 13.85]
	Operational performance																		
	W_{CCE} (boxes)	63	[46; 79]	173	[141; 205]	243	[208; 277]	313	[279; 347]	449	[405; 492]	463	[417; 510]	373	[331; 415]	380	[336; 423]	396	[352; 440]
	W_{tr} (boxes)	2139	[2120; 2158]	2324	[2307; 2341]	2401	[2379; 2422]	1996	[1982; 2010]	2060	[2043; 2077]	2096	[2081; 2112]	1589	[1579; 1600]	1604	[1593; 1614]	1609	[1597; 1620]
	MO_{inv} (boxes)	15314	[13750; 16878]	14717	[13285; 16149]	20544	[18146; 22942]	15191	[14300; 16083]	23615	[22228; 25003]	32442	[31304; 33580]	19702	[19238; 20165]	31677	[30963; 43019]	43019	[42093; 43945]
	MO_{veh} (boxes)	8694	[8049; 9338]	9462	[8777; 10147]	9922	[9203; 10641]	1289	[1012; 1567]	1213	[911; 1514]	1379	[1029; 1729]	199	[104; 294]	214	[105; 324]	201	[60; 343]
	MO_{cap} (boxes)	1656	[1575; 1737]	2854	[2709; 2998]	5053	[4833; 5274]	8446	[8175; 8716]	16376	[15984; 16767]	22704	[22238; 23171]	26631	[26264; 26997]	34307	[33832; 34783]	39431	[38910; 39951]

References

Aina, M., U. Igbokwe, L. Jegede, R. Fagge, A. Thompson, and N. Mahmoud (2017). Preliminary results from direct-to-facility vaccine deliveries in Kano, Nigeria. *Vaccine 35*(17), 2175–2183.

Ajin, R. S., R. R. Krishnamurthy, M. Jayaprakash, and P. G. Vinod (2013). Flood hazard assessment of Vamanapuram river basin , Kerala , India : An approach using remote sensing and GIS techniques. *Advances in Applied Science Research 4*(3), 263–274.

Ares, J. N., H. de Vries, and D. Huisman (2016). A column generation approach for locating roadside clinics in Africa based on effectiveness and equity. *European Journal of Operational Research 254*(3), 1002–1016.

Ashok, A., M. Brison, and Y. LeTallec (2017). Improving cold chain systems: Challenges and solutions. *Vaccine 35*(17), 2217–2223.

Assi, T.-M. (2011). *Impacts of vaccine cold chain logistics on vaccine epidemiology.* Ph. D. thesis, University of Pittsburgh.

Assi, T.-M., S. Brown, S. Kone, B. Norman, A. Djibo, D. L. e. a. Connor, A. R. Wateska, J. Rajgopal, R. B. Slayton, and B. Y. Lee (2013). Re-moving the regional level from the Niger vaccine supply chain. *Vaccine 31*(26), 2828–2834.

Berenguer, G., A. V. Iyer, and P. Yadav (2016). Disentangling the efficiency drivers in country-level global health programs: An empirical study. *Journal of Operations Management 45*, 30–43.

Brooks, A., D. Habimana, and G. Huckerby (2017). Making the leap into the next generation: A commentary on how GAVI, the vaccine alliance is supporting countries' supply chain transformations in 2016-2020. *Vaccine 35*(17), 2110–2114.

Brown, S. T., B. Schreiber, B. E. Cakouros, A. R. Wateska, H. M. Dicko, D. L. Connor, P. Jaillard, M. Mvundura, B. A. Norman, C. Levin, J. Rajgopal, M. Avella, C. Lebrund, E. Claypool, P. Paul, and B. Y. Lee (2014). The benefits of redesigning Benin's vaccine supply chain. *Vaccine 32*(32), 4097–4103.

Broxton, P. D., X. Zeng, D. Sulla-Menashe, and P. A. Troch (2014). A global land cover

climatology using MODIS data. *Journal of Applied Meteorology and Climatology 53*, 1593–1605.

CGIAR-CSI (2019). SRTM 90m DEM digital elevation database. Retrieved from http://srtm.csi.cgiar.org.

Cherkesly, M., M.-E. Rancourt, and K. R. Smilowitz (2019). Community healthcare network in underserved areas: Design, mathematical models, and analysis. *Production and Operations Management 28*(7), 1716–1734.

Climate-ADAPT (2019). Oasishub (2017). Retrieved from https://climate-adapt.eea.europa.eu/metadata/portals/oasishub.

De Boeck, K., C. Decouttere, and N. Vandaele (2019). Vaccine distribution chains in low- and middle-income countries: A literature review. *Omega*.

de Treville, S., I. Smith, A. Rölli, and V. Arnold (2006). Applying operations management logic and tools to save lives: A case study of the World Health Organization's global drug facility. *Journal of Operations Management 24*(4), 397–406.

de Vries, H., J. van de Klundert, and A. P. M. Wagelmans (2020). The roadside healthcare facility location problem: A managerial network design challenge. *Production and Operations Management*.

Decouttere, C., K. De Boeck, and N. Vandaele (2020). Immunization operations within a Sustainable Development Goals' strategy: A literature review. Working paper.

Demographic and Health Surveys Program (2019). Retrieved from https://dhsprogram.com/.

Deo, S. and M. Sohoni (2015). Optimal decentralization of early infant diagnosis of HIV in resource-limited settings. *Manufacturing & Service Operations Management 17*(2), 191–207.

Dewilde, S. (2018). Cold chain distribution network design in developing countries - A robust and resilient vaccine distribution network in Madagascar. Master's thesis, KU Leuven.

Doerner, K., A. Focke, and W. J. Gutjahr (2007). Multicriteria tour planning for mobile healthcare facilities in a developing country. *European Journal of Operational Research 179*(3), 1078–1096.

Earth Engine Data Catalog (2019). Global friction surface 2015. Retrieved from https://developers.google.com/earth-engine/datasets/catalog/Oxford_MAP_friction_surface_2015_v1_0.

Fick, S. E. and R. J. Hijmans (2017). Worldclim 2: New 1-km spatial resolution climate surfaces for global land areas. *International Journal of Climatology 37*(12), 4302–4315.

Gallien, J., I. Rashkova, R. Atun, and P. Yadav (2017). National drug stockout risks and the Global Fund disbursement process for procurement. *Production and Operations Management 26*(6), 997–1014.

Haidari, L. A., S. T. Brown, M. Ferguson, E. Bancroft, M. Spiker, A. Wilcox, R. Ambikapathi, V. Sampath, D. L. Connor, and B. Y. Lee (2016). The economic and operational value of using drones to transport vaccines. *Vaccine 34*(34), 4062–4067.

Hao, P., Z. Sun, X. Ban, D. Guo, and Q. Ji (2013). Vehicle index estimation for signalized intersections using sample travel times. *Transportation Research Part C: Emerging Technologies 36*, 513–529.

Heaton, A., K. Krudwig, T. Lorenson, C. Burgess, A. Cunningham, and R. Steinglass (2017). Doses per vaccine vial container: An understated and underestimated driver of performance that needs more evidence. *Vaccine 35*(17), 2272–2278.

Herlin, H. and A. Pazirandeh (2012). Nonprofit organizations shaping the market of supplies. *International Journal of Production Economics 139*(2), 411–421.

James, W., N. Tejedor-Garavito, S. E. Hanspal, A. Campbell-Sutton, G. M. Hornby, C. Pezzulo, K. Nilsen, A. Sorichetta, C. W. Ruktanonchai, A. Carioli, D. Kerr, Z. Matthews, and A. Tatem (2018). Gridded birth and pregnancy datasets for Africa, Latin America and the Caribbean. *Scientific Data 5*.

Jónasson, J., S. Deo, and J. Gallien (2017). Improving HIV early infant diagnosis supply chains in sub-Saharan Africa: Models and application to Mozambique. *Operations Research 65*(6), 1479–1493.

Karp, C., D. Lans, J. Esparza, E. Edson, K. Owen, C. Wilson, P. M. Heaton, O. S. Levine, and R. Rao (2015). Evaluating the value proposition for improving vaccine thermostability to increase vaccine impact in low and middle-income countries. *Vaccine 33*(30), 3471–3479.

Kourgialas, N. N. and G. P. Karatzas (2011). Flood management and a GIS modelling method to assess flood-hazard areas - A case study. *Hydrological Sciences Journal - Journal des Sciences Hydrologiques 56*(2), 212–225.

Kraiselburd, S. and P. Yadav (2012). Supply chains and global health: An imperative for bringing operations management scholarship into action. *Production and Operations Management 22*(2), 337–381.

KTH-dESA (2019). Madagascar - slope. Retrieved from https://energydata.info/dataset/madagascar-slope-2017.

LCA (2019a). LCA Homepage. Retrieved from https://dlca.logcluster.org/display/public/DLCA/LCA+Homepage.

LCA (2019b). Madagascar road network. Retrieved from https://dlca.logcluster.org/display/public/DLCA/2.3+Madagascar+Road+Network.

Lemmens, S., C. Decouttere, N. Vandaele, and M. Bernuzzi (2016). A review of integrated supply chain network design models: Key issues for vaccine supply chains. *Chemical Engineering Research and Design 109*, 366–384.

Lennon, P., B. Atuhaire, S. Yavari, V. Sampath, M. Mvundura, N. Ramanathan, and J. Robertson (2017). Root cause analysis underscores the importance of understanding, addressing, and communicating cold chain equipment failures to improve equipment performance. *Vaccine 35*(17), 2198–2202.

Leung, N., A. Chen, P. Yadav, and J. Gallien (2016). The impact of inventory management on stock-outs of essential drugs in sub-Saharan Africa: Secondary analysis of a field experiment in Zambia. *PLoS ONE 11*(5), e0156026.

Madagascar Decision Support System (2019). Madagascar Decision Support System: Infrastructure sanitaire: Centre de santé. Retrieved from http://snisnet.net/MDDSS/MDDSS.htm.

Mazloumi, E., G. Currie, and G. Rose (2010). Using GPS data to gain insight into public transport travel time variability. *Journal of Transportation Engineering 136*(7), 623–631.

Mccoy, J. H. and E. M. Johnson (2014). Clinic capacity management: Planning treatment programs that incorporate adherence. *Production and Operations Management 23*(1), 1–18.

McCoy, J. H. and H. L. Lee (2014). Using fairness models to improve equity in health delivery fleet management. *Production and Operations Management 23*(6), 965–977.

Mehrotra, M. and K. V. Natarajan (2019). Value of combining patient and provider incentives in humanitarian health care service programs. *Production and Operations Management*.

Morgan, R. P. C. (2005). *Soil erosion and conservation*. Oxford: Blackwell Publishing Ltd.

Natarajan, K. V. and J. M. Swaminathan (2014). Inventory management in humanitarian operations: Impact of amount, schedule, and uncertainty in funding. *Manufacturing & Service Operations Management 16*(4), 595–603.

Natarajan, K. V. and J. M. Swaminathan (2017). Multi-treatment inventory allocation in humanitarian health settings under funding constraints. *Production and Operations Management 26*(6), 1015–1034.

OasisHub (2019). Categorised flood hazard map of Madagascar. Retrieved from https://oasishub.co/dataset/madagascar-categorised-flood-hazard-fathom/resource/da098853-8e9e-4d38-b079-f9216397364a?inner_span=True.

Ozkan, S. P. and C. Tarhan (2016). Detection of flood hazard in urban areas using GIS: Izmir case. *Procedia Technology 22*, 373–338.

Parvin, H., S. Beygi, J. E. Helm, P. S. Larson, and M. P. Van Oyen (2017). Distribution of medication considering information, transshipment, and clustering: Malaria in Malawi. *Production and Operations Management 27*(4), 774–797.

Rabta, B., C. Wankmüller, and G. Reiner (2018). A drone fleet model for last-mile distribution in disaster relief operations. *International Journal of Disaster Risk Reduction 28*, 107–112.

Rajgopal, J., D. L. Connor, T.-M. Assi, B. A. Norman, S.-I. Chen, R. R. Bailey, A. R. Long, A. R. Wateska, K. M. Bacon, S. T. Brown, D. S. Burke, and B. Y. Lee (2018). The optimal number of routine vaccines to order at health clinics in low- or middle-income countries. *Vaccine 29*(33), 5512–5518.

Restrepo-Méndez, M. C., A. J. D. Barros, K. L. M. Wong, H. L. Johnson, G. Pariyo, G. V. A. França, F. C. Wehrmeister, and C. G. Victora (2016). Inequalities in full immunization coverage: Trends in low- and middle-income countries. *Bulletin of the World Health Organization 94*(11), 794–805A.

Shaban, A., M. Khawlie, R. Bou Kheir, and C. Abdallah (2001). Assessment of road instability along a typical mountainous road using GIS and aerial photos. *Bulletin of Engineering Geology and the Environment 60*(2), 93–101.

Smith, H. K., P. R. Harper, C. N. Potts, and A. Thyle (2009). Planning sustainable community health schemes in rural areas of developing countries. *European Journal of Operational Research 193*(3), 768–777.

Srinivasan, K. K., A. A. Prakash, and R. Seshadri (2014). Finding most reliable paths on networks with correlated and shifted log-normal travel times. *Transportation Research Part B 66*, 110–128.

Tatem, A., J. Campbell, M. Guerra-Arias, L. de Bernis, A. Moran, and Z. Matthews (2014). Mapping for maternal and newborn health: The distributions of women of childbearing age, pregnancies and births. *International Journal of Health Geographics 13*(2).

Taylor, T. A. and W. Xiao (2014). Subsidizing the distribution channel: Donor funding to improve the availability of malaria drugs. *Management Science 60*(10), 2461–2477.

UN (2019a). Sustainable Development Goal 13. Retrieved from https://sustainabledevelopment.un.org/sdg13.

UN (2019b). Sustainable Development Goal 3. Retrieved from https://sustainabledevelopment.un.org/sdg3.

USAID (2017). Madagascar — U.S. Agency for International Development. Retrieved from https://www.usaid.gov/madagascar.

van den Ent, M. M. V. X., A. Yameogo, E. Ribaira, C. M. Hanson, R. Ratoto, S. Rasolomanana, C. Foncha, and F. Gasse (2017). Equity and immunization supply chain in Madagascar. *Vaccine 35*(17), 2148–2154.

Van Hout, D. (2019). GIS and spatial models for vaccine distribution in remote areas. Master's thesis, KU Leuven.

Vandaele, N. (1996). *The impact of lot sizing on queueing delays: Multi Product, multi machine models*. Ph. D. thesis, KU Leuven.

Verdin, K. (2017). Hydrologic Derivatives for Modeling and Applications (HDMA) database: U.S. geological survey data release.

Wallace, A., F. Willis, E. Nwaze, B. Dieng, N. Sipilanyambe, D. Daniels, E. Abanida, A. Gasasira, M. Mahmud, and T. K. Ryman (2017). Vaccine wastage in Nigeria: An assessment of wastage rates and related vaccinator knowledge, attitudes and practices. *Vaccine 35*(48), 6751–6758.

Weiss, D. J., A. Nelson, H. S. Gibson, W. Temperley, S. Peedell, A. Lieber, M. Hancher, E. Poyart, S. Belchior, N. Fullman, B. Mappin, U. Dalrymple, J. Rozier, T. C. D. Lucas, R. E. Howes, L. S. Tusting, S. Y. Kang, E. Cameron, D. Bisanzio, K. E. Battle, S. Bhatt, and P. W. Gething (2018). A global map of travel time to cities to assess inequalities in accessibility in 2015. *Nature 553*(7688), 333–336.

WHO (2014). WHO policy statement: Multi-dose vial policy (MDVP). Retrieved from https://apps.who.int/iris/bitstream/handle/10665/135972/WHO_IVB_14.07_eng.pdf;jsessionid=27D98A8C2E992AD961C5CF8E2D4E44DA?sequence=1.

WHO (2017, July). Immunization coverage: Fact sheet. Retrieved from http://www.who.int/mediacentre/factsheets/fs378/en/.

WHO (2018, February). Climate change and health. Retrieved from https://www.who.int/news-room/fact-sheets/detail/climate-change-and-health.

WHO/UNICEF (2017, July). Progress towards global immunization goals - 2016: Summary presentation of key indicators. Retrieved from http://apps.who.int/gho/cabinet/gvap.jsp.

WHO/UNICEF (2018). Madagascar: WHO and UNICEF estimates of immunization coverage: 2018 revision. Retrieved from https://www.who.int/immunization/monitoring_surveillance/data/mdg.pdf.

World Bank (2015). Madagascar systematic country diagnostic. Retrieved from http://documents.worldbank.org/curated/en/743291468188936832/pdf/99197-CAS-P151721-IDA-SecM2015-0168-IFC-SAecM2015-0123-Box393189B-OUO-9.pdf.

World Bank (2019a). The World Bank in Madagascar: Overview. Retrieved from https://www.worldbank.org/en/country/madagascar/overview.

World Bank (2019b). World Bank supports Madagascar's efforts to reduce disaster risk with $50 million. Retrieved from https://www.worldbank.org/en/news/press-release/2019/12/12/world-bank-supports-madagascars-efforts-to-reduce-disaster-risk-with-50-million.

World Economic Forum (2017). Global competitiveness report 2017-2018 Madagascar. Retrieved from http://reports.weforum.org/pdf/gci-2017-2018/WEF_GCI_2017_2018_Profile_MDG.pdf.

Worldpop (2019). Madagascar 1km births. Retrieved from https://www.worldpop.org/geodata/summary?id=848.

FACULTY OF ECONOMICS AND BUSINESS
Naamsestraat 69 bus 3500
3000 LEUVEN, BELGIË
tel. + 32 16 32 66 12
fax + 32 16 32 67 91
info@econ.kuleuven.be
www.econ.kuleuven.be